1   # The influence of multiple salt layers on rift-basin

2   # development; The Slyne and Erris basins, offshore NW

3   # Ireland

4   Conor M. O'Sullivan [1, 2], Conrad J. Childs [1, 2], Muhammad M. Saqab [1, 2*], John J. Walsh [1, 2],

5   Patrick M. Shannon [1, 3]

6   [1] Irish Centre for Research in Applied Geoscience (iCRAG), University College Dublin, Belfield, Dublin 4, Ireland

7   [2] Fault Analysis Group, School of Earth Sciences, University College Dublin, Belfield, Dublin 4, Ireland

8   [3] School of Earth Sciences, University College Dublin, Belfield, Dublin 4, Ireland

9   [*]Present Address: Norwegian Geotechnical Institute, 40 St. Georges Terrace, Perth, WA 6000, Australia

10   Corresponding author email: conor.osullivan@icrag-centre.org

11   ## Abstract:

12   In contrast to much of the European Atlantic margin, the influence of salt on basin evolution

13   has received little attention to date in the basins west of Ireland, despite salt being proven in

14   several boreholes. Using an extensive seismic reflection database coupled with data from

15   exploration wells and shallow boreholes, this study maps the distribution and composition of

16   salt layers and investigates their role in the structural evolution of the Slyne and Erris basins

17   offshore west of Ireland. Two salt-prone intervals have been proven. The Upper Permian

18   Zechstein Group is present throughout the Slyne and Erris basins, while the Upper Triassic

19   Uilleann Halite Member is only developed in the Northern Slyne and Southern Erris sub-

20   basins. Both sedimentary units mechanically detach pre-, post-, and intra-salt stratigraphy.

21   Both salt layers underwent halokinesis during basin development, creating a variety of salt-

22   related structures. Salt pillows and salt rollers formed in the Zechstein Group, causing folding

23   and rafting in the overlying Mesozoic section, driven by active faulting within the pre-salt

24   basement. Halokinesis in the Uilleann Halite Member caused thin-skinned crestal collapse of

25   the overlying Jurassic section above anticlines cored by Zechstein salt. Where both Triassic

26   and Permian salt are present, unique structural geometries are formed when two

27   stratigraphically discrete but kinematically linked halokinetic structures develop. The most

28   common structural configuration consists of a Zechstein salt pillow and an Uilleann Halite salt

29   wall separated by Lower Triassic sandstones. The fold-axis of the salt pillow trends parallel to

30   the strike of the salt wall. The results of this study provide a framework for the evolution of

31   halokinetic structures in other basins on the Irish Atlantic margin, give a greater insight into

32   the Permian and Triassic paleogeography of the region, and have more general implications

33 for the evolution of salt-related structures in rift basins with multiple stratigraphically discrete

34 salt layers.

35 Highlights

36 • Upper Permian and Upper Triassic salt layers present in the Slyne and Erris basins.

37 • Zechstein Group forms salt pillows and reactive diapirs, Uilleann Halite forms

38 reactive diapirs.

39 • Even thin salt layers act as prominent décollement surfaces during rifting.

40 • Stratigraphically discrete salt layers interact during structural evolution.

Acknowledgements

Data Availability Statement

The data that support the findings of this study were provided by the Petroleum Affairs Division (PAD) and are available for download from https://www.dccae.gov.ie/en-ie/natural-resources/topics/Oil-Gas-Exploration-Production/data/Pages/Data.aspx. Restrictions may apply to the availability of these data, which were used under licence for this study.

1. Introduction:

Salt plays an important role in the development of sedimentary basins, acting as a layer of mechanical detachment between pre- and post-salt stratigraphy (Hudec & Jackson, 2007; Jackson & Hudec, 2017b). This leads to significant differences in the structural styles and evolution of salt-influenced basins relative to those unaffected by salt. Thick layers of salt have been encountered in several basins across the European Atlantic margin, including offshore Iberia (Wilson et al., 1989; Alves et al., 2006; Pena dos Reis et al., 2017; Ramos et al., 2017; Zamora et al., 2017), offshore France (Chapman, 1989; Ferrer et al., 2012), on the United Kingdom Continental Shelf (UKCS) (Stewart et al., 1996; Jackson & Stewart, 2017) and offshore Norway (Jackson et al., 2019; Rojo et al., 2019). Salt is also present in basins on the conjugate margin of Atlantic Canada (Jansa et al., 1980; Deptuck & Kendell, 2017). In these areas, the main layers of salt range in age from Early Permian to Early Jurassic, and have had a profound impact on basin development, commonly having undergone significant halokinesis to form distinctive salt-related structures such salt diapirs and allochthonous salt sheets and canopies (McKie, 2017; Stoker et al., 2017).

The Irish Atlantic margin has seen comparatively little research investigating the presence and impact of salt, owing to the limited well penetrations and lack of characteristic salt-related structures on seismic data. Nevertheless, Upper Triassic salt is proven in the Celtic Sea basins (Robinson et al., 1981; Van Hoorn, 1987; Shannon, 1991), the Central Irish Sea and St George's Channel basins (Naylor & Shannon, 1982) and the Kish Bank Basin (Naylor et al., 1993; Dunford et al., 2001). In the Porcupine Basin, Croker & Shannon (1987) reported the presence of salt in two wells in the north of the basin, while the 35/19-1 well encountered 24m of ?Upper Triassic allochthonous salt within Upper Jurassic sediments (Britoil, 1986; Merlin Energy Resources Consortium, 2020). Salt has also been identified onshore Ireland, within the Ulster-Larne Basin of Northern Ireland (Illing & Griffith, 1986; McCann, 1988; Quinn et al., 2010) and in a small outlier at Kingscourt, Co. Cavan (Gardiner & Visscher, 1971; Gardiner & McArdle, 1992). Previous work has noted the presence of salt in the Slyne and Erris basins (Tate & Dobson, 1989; Chapman et al., 1999; Dancer et al., 1999; Dancer et al., 2005) but limited and poor-quality seismic data, coupled with few well penetrations, made it difficult to assess the impact of these salt-prone layers on basin development. Since then, significantly more seismic data has been acquired and additional exploration wells have been drilled, allowing the nature of salt and the role it plays in the evolution of the Slyne and Erris basins to be investigated in greater detail (Fig. 1).

This study utilizes an extensive database of 2D and 3D multichannel seismic reflection data, coupled with wireline, cuttings and core data from exploration wells and shallow boreholes to

98   understand the distribution and composition of salt in the Slyne and Erris basins, and the
99   impact of salt on the structural evolution of these basins. Both Upper Permian (Zechstein
100   Group) and Upper Triassic (Uilleann Halite Member) salt layers have now been identified over
101   significant parts of the study area. The Uilleann Halite Member was referred to as the Mercia
102   Halite Member (e.g. Corcoran & Mecklenburgh, 2005; Dancer et al., 2005) prior to recent
103   updates to the stratigraphic framework for offshore Ireland (Merlin Energy Resources
104   Consortium, 2020). The occurrence of two salt layers results in stacked salt-related structures
105   with evidence for interaction between halokinetic features developed at different structural
106   levels.

107   In our study the distribution of salt on the Irish Atlantic margin is placed in regional context to
108   provide insights into Late Permian and Late Triassic paleogeography of the north-western
109   European Atlantic margin. The influence of salt on the petroleum systems of the Slyne and
110   Erris basins is also discussed. The evolutionary model for halokinetic structures involving
111   multiple thin salt layers may be applicable to other rift basins beyond the Irish Atlantic margin,
112   particularly across NW Europe where several basins have multiple, stratigraphically discrete
113   layers of salt.

2. Geological Setting:

The Slyne and Erris basins are contiguous rift basins located on the Irish Mainland Shelf off the north-western coast of Ireland in water depths of 150m to 3000m. They are narrow, elongate and broadly NE-SW oriented basins, which belong to a framework of rift basins extending westward from the coast of Ireland across the Irish Atlantic margin to the Atlantic Abyssal Plain. They form part of chain of rift basins stretching along the European Atlantic margin from the Barents Sea offshore northern Norway to offshore Portugal (Fig. 1). These rift basins formed during episodic extensional periods beginning with Variscan orogenic collapse and culminating with the onset of oceanic crust formation in the North Atlantic Ocean during the Eocene (Doré et al., 1999, Stoker et al., 2017; Schiffer et al., 2019).

2.1. Tectonostratigraphic evolution of the Slyne and Erris basins:

The Slyne and Erris basins began to form during the Permian breakup of Pangea. Extension created a series of narrow, NE-SW and NNE-SSW oriented half-grabens (Fig. 1; Chapman et al., 1999; Dancer et al., 1999). The arid Permian climate led to the deposition of the Zechstein Supergroup, a large and widely studied 'salt giant' present across north-western Europe (Coward, 1995; Stewart, 2007; Duffy et al., 2013; Jackson & Stewart, 2017). This salt body formed through the ingress and subsequent evaporation of marine waters from the Boreal Ocean to the north (McKie, 2017). Possible pathways connecting the Irish Atlantic margin and the Boreal Ocean include the Faroe-Shetland Basin, the Hebridean basins, and an incipient Rockall rift system (Štolfová & Shannon, 2009; McKie & Shannon, 2011; McKie, 2017). Extension ceased by the Early Triassic, with thick fluvial and aeolian sandstones being deposited regionally, followed by the widespread deposition of playa-lake mudstones and siltstones and locally thick halite deposits during the Late Triassic (Štolfová & Shannon, 2009; Merlin Energy Resources Consortium, 2020).

The end of the Triassic was marked by a regional marine transgression and the deposition of shallow marine limestones, sandstones and mudstones during the Rhaetian to the Sinemurian (Trueblood & Morton, 1991; Raine et al., 2020). The area experienced mild extension during this time, with subtle syn-extensional thickening of the Lower Jurassic section occurring in the hanging-walls of active basin-bounding faults (Dancer et al., 1999). Intrabasinal NE-SW and NNE-SSW striking listric faults formed throughout the basin above small salt rollers and salt pillows. A minor break during the early Pliensbachian created a subtle unconformity, above

146   which Late Pliensbachian to Bajocian marine sandstones, limestones and mudstones were
147   deposited.

148   A major unconformity separates the Lower and Middle Jurassic marine sediments from the
149   overlying Upper Jurassic fluvio-estuarine sediments, with the unconformity locally incising
150   deeply enough to place the Oxfordian above the Pliensbachian and Sinemurian on the basin
151   margins. The main phase of rifting occurred during this time, with movement on basin-
152   bounding faults creating accommodation space for the deposition of several kilometres of
153   Upper Jurassic sediments (Merlin Energy Resources Consortium, 2020). The Upper Jurassic
154   sediments consist of Oxfordian terrestrial, fluvial and estuarine sandstones and mudstones
155   with associated coal horizons, which grade upwards into marine mudstones, limestones and
156   sandstones, indicating a regional marine transgression occurred during the Kimmeridgian and
157   Tithonian (Fig. 2).

158   Rifting in the Slyne and Erris basins ceased at the end of the Jurassic, with the area
159   experiencing kilometre-scale uplift and erosion during the Early Cretaceous. As rifting
160   occurred in the Rockall Basin to the west, the Erris Basin in particular was subject to severe
161   rift-shoulder uplift, undergoing greater uplift along the western margin of the basin while thick
162   Cretaceous sediments were deposited along the basin's eastern margin (Chapman et al.,
163   1999; Walsh et al., 1999). Areas that were separated from the Rockall Basin by intervening
164   basement highs, such as the Erris Ridge, did not experience the same extent of rift-shoulder
165   uplift. The Slyne Basin remained a relative high throughout the Cretaceous, shielded from rift-
166   related subsidence in the Rockall Basin by the Porcupine High, with only a thin veneer of
167   Lower and Upper Cretaceous sediments deposited throughout the basin.

168   As rifting in the Rockall Basin ceased towards the end of the Cretaceous, the basin underwent
169   thermal subsidence, with the western margins of the northern Slyne and the Erris basins that
170   had been subject to rift-shoulder uplift now experiencing kilometre-scale subsidence. Post-rift
171   tectonic activity continued throughout the Paleocene, Eocene and Early Miocene, expressed
172   as subtle normal and reverse movement on faults throughout the basins, and in the formation
173   of E-W oriented strike-slip faults, likely related to along-strike movement on major Caledonian
174   crustal lineaments like the Great Glen and Fair Head-Clew Bay lineaments (Cooper et al,
175   2012; Le Breton et al., 2013; Anderson et al., 2018). The development of the North Atlantic
176   Igneous Province during the mid-Eocene had an impact on the Slyne and Erris basins, with
177   the intrusion of several sills into the Mesozoic basin-fill and the extrusion of thick basaltic lavas
178   of the Druid Formation (Jolley & Bell, 2002). These layered basalt flows are thickest on the
179   western margin of the Southern Slyne Sub-basin, the Northern Slyne Sub-basin and in the

180 Northern Erris Sub-basin, where they degrade the quality of seismic data beneath these
181 volcanic layers (Dancer & Pillar, 2001).

182 ## 2.2. Structural Framework & Basin Morphology

183 The Irish Mainland Shelf separates the Slyne and Erris basins from the island of Ireland to the
184 southeast, while the Rockall Basin bounds the Erris Basin along its north-western margin, with
185 the Slyne and Porcupine highs bounding the Slyne Basin along its western margin (Fig. 1).
186 The Erris Ridge is a NE-SW oriented, discontinuous basement high that separates the Rockall
187 Basin from the Erris Basin and the northern Slyne Basin (Cunningham & Shannon, 1997). The
188 Porcupine Basin is located to the southwest of the Slyne Basin and separated from it by a
189 narrow basement horst.

190 The present-day morphology of the Slyne and Erris basins is largely controlled by their location
191 on the Irish Continental Shelf and the development of the neighbouring Rockall Basin; the
192 seabed above the Slyne Basin is topographically flat with no bathymetric expression, while
193 the Erris Basin dips westwards along the shelf break into the Rockall Basin. This dip is more
194 subtle in the Northern Erris Sub-basin, where the Erris Ridge is present, and more pronounced
195 in the Southern Erris Sub-basin, beyond the extent of the Erris Ridge. The Erris Basin is
196 transected by several present-day canyon systems that feed into the Rockall Basin from the
197 Irish Mainland Shelf.

198 The Slyne and Erris basins are transected by several crustal-scale structural lineaments (Fig.
199 1), representing suture zones and terrane boundaries separating Caledonian and Pre-
200 Cambrian basement terranes that were accreted during the Grenville and Caledonian
201 orogenies (Chew & Stillman, 2009). These structural lineaments trend NE-SW across onshore
202 Ireland, rotating to trend E-W as they continue westwards into the offshore domain (Hutton &
203 Alsop, 1996). Younger Mesozoic rift basins are segmented where the cross these Caledonian
204 lineaments to form sub-basins that exhibit differences in structural style and geology and that
205 are separated by structural complex transfer zones (Fig. 1; Trueblood, 1992; Dancer et al.,
206 1999). The Slyne Basin can be subdivided into three distinct sub-basins, the Southern,
207 Central, and Northern Slyne sub-basins. The offshore extension of the Fair Head-Clew Bay
208 lineament separates the Southern and Central Slyne sub-basins, while the offshore extension
209 of the Great Glen Fault Zone separates the Central and Northern Slyne sub-basins (Fig. 1;
210 Dancer et al., 1999). The Erris Basin has previously been subdivided into three sub-basins
211 based on the predominant dip of the faults in the Mesozoic section (e.g. Chapman et al., 1999);
212 for the purposes of this study the Northern and Central Erris sub-basins of previous literature
213 have been combined.

3. Dataset and Methodology:

This study utilises an extensive, multi-vintage seismic dataset covering the majority of the Slyne and Erris basins as well as extending into neighbouring regions (Fig. 3). The seismic database contains both 2D and 3D seismic reflection data. The 2D database consists of 25 surveys, acquired between 1975 and 2014 that total over 49,000 km in line-length. The 3D database comprises 12 seismic surveys with a total area of over 6000 km^2, although there is a significant area of overlap in the Northern Slyne Sub-basin. Most of the 3D surveys were acquired between 1997 and 2003, with the 1997 Corrib 3D (Dancer & Pillar, 2001) reprocessed in 2006, 2012 and 2018. Seismic quality in the Slyne and Erris basins varies from very poor to good and is dependent on the near-seabed geology. Extensive Eocene volcanics of the Druid Formation extruded during the formation of the North Atlantic Igneous Province, as well as exceptionally hard limestones of the Upper Cretaceous Chalk Group cause widespread imaging problems, principally multiple generation, energy scattering and signal attenuation (Dancer & Pillar, 2001). The volcanics are thickest in the Northern Slyne Sub-basin and the Southern Erris Sub-basin, as well as atop the Erris Ridge, while the Chalk Group is present throughout the Erris Basin and in the Northern Slyne Sub-basin. Seismic resolution varies across the study area due to different frequencies used by individual seismic surveys. In general, the vertical seismic resolution used for identifying salt layers varies between 10-20 m near the seabed to 70-120 m at c. 5 km below the seabed (one-quarter wavelength sensu Brown, 2011). Seismic sections are presented in European polarity (Brown, 2001), where a positive downwards increase in acoustic impedance corresponds to a positive (red) reflection event and a decrease corresponds to a negative (blue) reflection event. All sections are vertically exaggerated by a factor of three. Ball-ends are used to highlight where a fault terminates within a certain stratigraphic package, while faults without ball-ends are truncated by a younger unconformity.

The seismic database was tied to released exploration and production wells and shallow boreholes across the study area. To date, two exploration wells have been drilled in the Erris Basin (19/5-1 and 12/13-1A), while eight exploration wells have been drilled in the Slyne Basin; these include the 18/20-1 Corrib gas discovery well, in addition to four near-field exploration wells in the Northern Slyne Sub-basin (19/8-1, 19/11-1A, 18/20-7, 18/25-2), with a further three exploration wells drilled in the Central Slyne Sub-basin (27/4-1, 27/5-1, 27/13-1). In addition to exploration wells, seven appraisal and production wells from the Corrib gas field are also incorporated into this study. The 27/13-1 well terminated in the Lower Jurassic, five other wells penetrated the Permian (12/13-1A, 19/5-1, 19/8-1, 18/25-2, and 27/5-1), with the remainder terminating in the Lower Triassic.

249   Exploration wells from neighbouring basins were also included to assess the distribution of
250   salt beyond the boundaries of the Slyne and Erris basins; these include the 12/2-1z and 12/2-
251   2 wells from the Rockall Basin, the 13/3-1 and 13/12-1 wells from the Donegal Basin, and the
252   26/22-1A, 26/21-1, 26/30-1 and 35/19-1A wells from the Porcupine Basin. The well database
253   is supplemented by three shallow boreholes; a single shallow borehole (11/20-sb01) drilled
254   on the crest of the Erris Ridge (Haughton et al., 2005), and two shallow boreholes (19/13-sb01
255   and 27/24-sb01) drilled in the Northern and Southern Slyne sub-basins respectively (Fugro,
256   1994). Data from the deep exploration wells include full suites of wireline logs (caliper, gamma,
257   density, neutron-porosity, resistivity, sonic), biostratigraphically-constrained formation tops,
258   cuttings descriptions, core photos, and time-depth relationships in the form of checkshots or
259   vertical seismic profiles (VSPs). The shallow borehole data include lithological descriptions,
260   formation tops, core photos, and select geochemical and geotechnical samples.

261   Evaporites in both the Late Triassic and Late Permian sections were identified using a
262   combination of wireline log data, cutting observations taken from both well completion reports
263   and composite logs, and core data, where available. With the relatively limited well database
264   available in the Slyne and Erris basins, the Permian and Late Triassic sections were sub-
265   divided simply; the Permian section was divided into three categories based on the proportion
266   of salt encountered, these being salt-dominated, transitional and clastic-dominated. Salt-
267   dominated sections are composed overwhelmingly of salt lithologies such as halite and
268   anhydrite, while clastic-dominated sections contain only sub-metre stringers of salt lithologies
269   in a background of sandstones, mudstones and carbonates. The transitional category contains
270   salt beds greater than a metre in thickness in a section largely composed of clastic and
271   carbonate lithologies. Stratigraphic sub-division has already been established for the Late
272   Triassic section, this being the presence or absence of the Uilleann Halite Member within the
273   Currach Formation (Fig. 2).

274   Seismic reflection data were used to map the extent of salt beyond areas where it has been
275   proven in borehole data. Halite mechanically detaches sub- and supra-salt sections, forming
276   distinct décollement surfaces on seismic sections, and can form distinct structures including
277   salt rollers, pillows and diapirs which can be used to indicate the presence of halite in the
278   section of interest (sensu Hudec & Jackson, 2007). Detailed seismic interpretation throughout
279   the Slyne and Erris basins alongside identification of salt-related structures therefore provided
280   a framework for mapping the distribution of both Permian and Triassic salt intervals within the
281   study area.

4. Salt Distribution and Composition:

Two layers of salt have been identified in the Slyne and Erris basins; the Zechstein Group, and the Uillean Halite Member within the Currach Formation. As well penetrations are relatively limited in the Slyne and Erris basins, seismic character was used to constrain the composition of salt-prone intervals away from areas with well-control.

4.1.   Zechstein Group

The Zechstein Group has been proven in all five exploration wells that penetrate the pre-Triassic section in the Slyne and Erris basins (12/13-1A, 19/5-1, 19/8-1, 18/25-2, 27/5-1), with variable lithologies encountered (Fig. 4). In the 12/13-1A in the Northern Erris Sub-basin, the Zechstein Group was largely composed of dolomite and anhydritic siltstones, with centimetre-scale stringers of anhydrite encountered throughout the section and reported from sidewall cores (Amoco, 1979). The Zechstein Group encountered in the 19/5-1 well in the Southern Erris Sub-basin and the 19/8-1 well in the Northern Slyne Sub-basin consisted of interbedded brown-red-grey mudstones and grey, microcrystalline dolomite accompanied by metre-scale stringers of anhydrite (Amoco, 1978; StatoilHydro, 2009). In the 18/25-2 well in the Northern Slyne Sub-basin, the Zechstein is composed of massive anhydrite alongside thin layers of microcrystalline dolomite and limestone at the top of the section, and thin layers of red-black mudstone towards the base of the sequence (Enterprise, 2000a). In the 27/5-1 well in the Central Slyne Sub-basin over 150 metres of massive halite was encountered, with thin magnesium salts encountered at the top of the section and interbedded anhydrite and claystone present towards the base of the section (Enterprise, 1996a). A 21-metre core was cut in the halite-prone section in the 27/5-1 well, described as white-pink-orange brittle halite (Fig. 4). These five well penetrations indicate a broad southward increase in the salt content of the Zechstein Group in the Slyne and Erris basins. Sediments belonging to the Zechstein Group may have been encountered at the base of some appraisal and production wells from the Corrib gas field; a mudstone-dominated section with minor anhydrite is present at the base of the Corrib Sandstone Formation in the 18/20-4 and 18/25-3 wells (Enterprise, 2000b, c). However, as these intervals are biostratigraphically barren (P. Copestake, pers. comm.) this remains unproven.

The variation in lithology of the Zechstein Group creates distinct wireline log profiles for both the salt-dominated and salt-poor forms. Salt-dominated sections have a characteristic blocky profile with low gamma ray values and high sonic velocities, while interbedded mudstone- and limestone-prone sections produces a more typical serrated wireline log character, higher gamma ray values and slower sonic velocities (Fig. 4).

When imaged on seismic data, the seismic response of the top Zechstein Group is often determined by the lithology at the base of the overlying Corrib Sandstone Formation. Where the Corrib Sandstone Formation is sandstone dominated towards the base, such as the Northern Slyne Sub-basin, a distinct negative impedance (blue) 'top-salt' reflector is observed (e.g. Fig. 5A, B). In areas where there is a greater proportion of mudstone and siltstone towards the base of the Corrib Sandstone Formation, such as the 27/5-1 well in the Central Slyne Sub-basin (Fig. 4), there is a less distinct 'top-salt' reflector (e.g. Fig. 6A). The unit itself is characterised by low-amplitude, bedded to chaotic reflectors, while local high-amplitude reflectors are occasionally observed and may represent clastic or carbonate bodies interbedded within halite-dominated areas (Fig. 7), although none of these high-amplitude bodies have been drilled to date. In areas of thinner, clastic-dominated Zechstein Group facies, the Permian section is often only represented by a single seismic wavelet (e.g. 19/5-1 well and seismic wavelet comparison in Figure 4).

Well penetrations and seismic data suggest the proportion of salt within the Zechstein Group decreases northwards, with only sub-metre scale stringers of anhydrite present in the 12/13-1A well, the most northerly in the basin (Fig. 1, 4). Seismic data from the undrilled Southern Erris Sub-basin suggests the presence of a salt-prone Permian section, where a distinct detachment surface is observed beneath the Triassic section.

4.2. Currach Formation & Uilleann Halite Member

The Upper Triassic Currach Formation has been encountered in every well in the Slyne and Erris basins, except the 18/25-2 well where the Upper Triassic succession was faulted out. The formation consists predominantly of red mudstone, locally accompanied by minor siltstone, limestone, dolomite and anhydrite. Towards the base of the formation, a series of metre-scale halite beds is present. In the Northern Slyne and Southern Erris sub-basins, a halite-dominated section, termed the Uilleann Halite Member, is developed at the base of the Currach Formation. This comprises brittle, crystalline white to pinkish grey halite (Enterprise, 1996b). The sediments of the Currach Formation reflect the arid lacustrine and sabkha conditions present in the Slyne and Erris basins during the Early Triassic, while the Uilleann Halite Member is indicative of a marine incursion into the Northern Slyne and Southern Erris sub-basins during the Middle to Late Triassic (Stoker et al., 2017).

The wireline log profiles of the Currach Formation consist of high gamma ray values and high sonic velocities associated with the mudstones that make up the bulk of the formation (Fig. 8). Interbedded siltstones, sandstones and carbonates typically have lower gamma ray values and slightly slower sonic velocities. The Uilleann Halite Member and smaller halite beds at the

base of the Currach Formation have very low gamma ray values and high sonic velocities, producing blocky wireline log profiles (Fig. 8). The Uilleann Halite Member is compositionally distinct from the Upper Permian salt, containing significantly more interbedded layers of red mudstone compared to the purer halite section in the Zechstein Group.

The top of the Currach Formation is marked by a high-amplitude soft or blue reflector on seismic data while the base of the formation is marked by a hard or red reflector representing the contact with the underlying Corrib Sandstone Formation (e.g. Fig. 5). The Currach Formation has a predominantly low-amplitude and chaotic seismic facies, with no clear distinction on seismic data with the Uilleann Halite Member. This is demonstrated in Figure 5B where the Upper Triassic section in the 18/20-7 well is predominantly red mudstone with only 13 metres of halite present while the 18/20-3 and 18/20-6 wells drilled a halite section over 600 metres thick (Fig. 8) with little seismic variation between the two well locations.

While the Currach Formation has been proven in every well except 18/25-2 for reasons described above, well data suggest the Uilleann Halite Member is restricted to the Northern Slyne Sub-basin. The Uilleann Halite Member has been proven in the wells associated with the Corrib gas field (blocks 18/20 and 18/25) in addition to 18/20-7, 19/11-1A and 19/8-1. No salt is present in the Currach Formation in either the 12/13-1A or 19/5-1 wells on the margins of the Erris Basin, while only very minor stringers of anhydrite were encountered in the 27/5-1 and 27/4-1 wells in the Central Slyne Sub-basin. The 27/13-1 well terminated at the base of the Lower Jurassic section, while the 27/24-sb02 shallow borehole in the Southern Slyne Sub-basin encountered sub-metre beds of gypsum towards the base of the Currach Formation (Fugro, 1994). Seismic data from the Southern Erris Sub-basin suggests the Uilleann Halite Member extends northwards into this part of the basin, with two detachment surfaces visible; the lower detachment occurring on the salt of the Zechstein Group, while the upper detachment occurs within the Uilleann Halite Member.

4.3.   Other salt-prone intervals in the Slyne & Erris basins

In addition to the Permian and Triassic salt present in the Slyne and Erris basins, several metres of anhydrite are interbedded with the sandstones, mudstones and limestones of the Lower Jurassic Meelagh Formation (Fig. 2). This anhydrite is developed in the Northern and Central Slyne sub-basins, with beds up to 20 metres thick encountered throughout the Meelagh Formation in the 18/20-1 well (Enterprise, 1996b), but thinning northwards, with no salt observed in the 19/11-1A well (Statoil, 2004). Only sub-metre-scale anhydrite stringers are recorded in the 19/8-1 well in the Northern Slyne Sub-basin, as well as the 19/5-1 and 12/13-1A wells in the Erris Basin (Amoco, 1978; Amoco, 1979; StatoilHydro, 2009). The

384 Meelagh Formation was deposited in an arid climate (Merlin Energy Resources Consortium,
385 2020), with the rapid vertical variation in facies representing an unstable and variable marginal
386 marine to marine environment. Like the salt-prone intervals in the Zechstein Group and
387 Uilleann Halite Member, the anhydrite beds within the Meelagh Formation have very low
388 gamma-ray values and high sonic velocities on wireline logs. There is no evidence of
389 mechanical detachment on the anhydrite beds of the Meelagh Formation seen on seismic
390 sections from the Slyne and Erris basins, although it is possible that local, sub-seismic bed-
391 parallel slip has occurred where these evaporites are present.

392 Within the Visean section of the 19/5-1 well in the Erris Basin, a sidewall core and cuttings at
393 2141 metres Measured Depth (mMD) are described as claystones containing stringers of
394 white anhydrite (Amoco, 1978). Gypsum has been encountered onshore Ireland in the
395 equivalent section in the Lough Allen Basin (Ambassador, 1962; Grennan, 1992). While this
396 section was only reached in a single well in the Erris Basin, it indicates the presence of salt-
397 prone strata at four discrete stratigraphic levels (Carboniferous, Upper Permian, Upper
398 Triassic, and Lower Jurassic) in the Slyne and Erris basins.

5. Salt structures in the Slyne and Erris basins

In areas of sparse well control, evidence of salt-related structures is supported by the identification of characteristic features on seismic data. The distribution and types of salt structures observed within the Slyne and Erris basins varies significantly between different sub-basins. This section analyses several of these structures and their implications for understanding salt composition and distribution.

5.1.   Southern and Central Slyne Sub-basins

In the south of the study area only the Zechstein Group is salt prone, whereas the Uilleann Halite Member is not developed within the Currach Formation. In this area the Zechstein Group acts as a décollement between the pre-salt basement and the post-salt Mesozoic section. The Southern and Central Slyne sub-basins are two contiguous half-graben which dip steeply westwards towards the basin-bounding fault running along their western margins, across which they are downthrown relative to the Porcupine High. The Central Slyne Sub-basin is downthrown relative to the Southern Slyne Sub-basin across the offshore extension of the Highland Boundary-Fair Head Clew Bay Lineament (Fig. 1).

In the Southern Slyne Sub-basin, a single, relatively large salt roller is identified in the centre of the sub-basin (Fig. 7). The Triassic, Lower Jurassic and Middle Jurassic sections dip more steeply north-westwards than both the underlying Carboniferous basement and the overlying Upper Jurassic section, with the Base Upper Jurassic Unconformity eroding the crest of the structure.

In the Central Slyne Sub-basin there are several high-relief, broadly anticlinal structures in the immediate hanging-wall of the bounding fault along the western margin of the basin (Fig. 6). While ostensibly similar, each structure exhibits subtle variations in geometry and composition. The Triassic to Middle Jurassic section penetrated in the 27/4-1 well in the immediate hanging-wall of the bounding fault was encountered at similar depths in the 27/5-1 well on the eastern margin of the Central Slyne Sub-basin (Fig. 6A). The Upper Jurassic section onlaps the steeply dipping eastern flank of the 27/4-1 structure, consistent with a predominately Late Jurassic age for the basin-bounding fault. The Upper Jurassic section also thickens eastwards into the hanging-wall of a major listric fault (Fig. 6A), indicating that movement on this fault occurred in tandem with the basin-bounding fault. The southern-most hanging-wall structure (Fig. 6B) is another high-relief anticlinal closure, with the Lower and Middle Jurassic section adjacent to the bounding-fault at a similar depth to the same section on the eastern margin of the basin. There is a distinct rotation of the Lower and Middle Jurassic

432   section facilitated by a detachment surface above the Triassic, suggesting the presence of
433   halite within the Currach Formation at this location.

434   Between these two high-relief structures there is a relative saddle abutting the basin-bounding
435   fault, forming a gently dipping dome. A distinct angular unconformity is observed beneath the
436   Upper Jurassic section (Fig. 6C) which is not observed at the crests of the structures along-
437   strike (Fig. 6A & B). Correlation from the 27/4-1 well indicates that the Middle Jurassic Kite
438   Group and a significant portion of the Lower Jurassic Lias Group, down to the Pabay
439   Formation, are absent from the crest of this saddle (Fig. 6C), while being preserved along-
440   strike at the higher relief 27/4-1 location (Fig. 6A). This indicates that this location was at a
441   higher relief relative to the present-day high-relief structures to the north and south during the
442   period of uplift and erosion that preceded Oxfordian rifting. This elevated area was likely to
443   have been cored by a gentle salt pillow before the emergence of the basin-bounding fault. As
444   the main phase of rifting initiated during the Oxfordian, the structures to the north and south
445   of this small salt pillow began to form, evidenced by onlap onto their flanks by the Upper
446   Jurassic section in this part of the basin.

447   Similar to the structure shown in Fig. 6C, a significant section of the Middle and Lower Jurassic
448   stratigraphy has been eroded from the eastern margin of the Central Slyne Sub-basin. The
449   Kite Group and part of the Lias Group, down to the Pabay Formation, are absent beneath the
450   base-Upper Jurassic unconformity in the 27/5-1 well while being present in the 27/4-1 well
451   (Fig. 6A). The base-Upper Jurassic unconformity is encountered at a relatively similar depth
452   present-day in both wells, 700 mMD and 845 mMD respectively (Merlin Energy Resources
453   Consortium, 2020), while having significantly different subcrops, highlighting the variation in
454   Zechstein Group salt topography during different extensional episodes.

455   The Central Slyne Sub-basin likely represents the erosional remnants of a significantly wider
456   basin that included the Slyne Embayment and a smaller disconnected half-graben to the west
457   of the Central Slyne Sub-basin (Fig. 1, 6A). The Slyne Embayment has a similar sedimentary
458   fill to that of the Central Slyne Sub-basin, with the Triassic and Jurassic sections overlying a
459   salt-prone Zechstein Group (Fig. 6A). Kilometre-scale erosion of the Jurassic section during
460   the Cretaceous and Cenozoic (Dancer et al., 1999; Biancotto et al., 2007) is interpreted to
461   have isolated the Slyne Embayment from the Central Slyne Sub-basin by eroding the footwall
462   of the bounding fault along the western margin of the Central Slyne Sub-basin (Fig. 6A).

5.2.   Northern Slyne Sub-basin

464   Several salt-cored folds are observed in the Northern Slyne Sub-basin, typically oriented NE-
465   SW and NNE-SSW, parallel to the syn-rift faults. Composed of Zechstein salt, these pillows

are between 5 to 15 kilometres in length and up to 10 kilometres wide, often flanked by salt withdrawal synclines which likely developed by salt movement into the pillows (Fig. 5). The folded Mesozoic stratigraphy above these salt pillows has been the target of several exploration wells in this part of the basin, including the 18/20-1 (Corrib), 18/20-7 and 19/11-1A wells (Fig. 5B, C). Changes in the thickness of the Jurassic section in the flanking synclines indicate that the polarity of these salt pillows varied during basin evolution. The Lower and Middle Jurassic section in the syncline to the NW of the Corrib anticline is thicker than the syncline to the SE, while a thicker Upper Jurassic section is observed in the SE syncline relative to the NW (Fig. 5B).

Several of these salt-cored folds have large delamination faults above their crests which sole out into the Uilleann Halite Member at the base of the Currach Formation. These faults are parallel to the axes of the salt-cored folds and are likely to have developed in tandem with the pillows of Permian salt, representing outer-arc extension and gravitational collapse at the apex of the salt-cored folds. These delamination faults are often accompanied by the formation of salt rollers in their footwalls (Fig. 5A, B), in addition to faulted rollovers in their hanging-walls.

These delamination faults have been reactivated at several stages during the Cretaceous and Cenozoic post-rift period; significant growth sequences in the Cretaceous section are observed in the hanging-walls of these large delamination faults, particularly in the Lower Cretaceous Spurdog Formation (Fig. 5A, B). The delamination faults also offset the top of the Druid Formation lavas and a portion of the overlying Cenozoic sediments, which are dated as 40-43 Ma in the 18/20-1 well (Dancer et al., 1999). The lack of folding in this Cretaceous and Cenozoic section indicates the later fault movement is more likely related to continued growth of the Upper Triassic salt roller rather than growth of the underlying Permian salt pillows and associated salt-cored folds.

5.3. Southern Erris Sub-basin

The Southern Erris Sub-basin dips steeply north-westwards as a result of post-rift thermal subsidence in the neighbouring Rockall Basin during the Cenozoic (Fig. 9-12). The western margin of the Erris Basin experienced significant rift-shoulder uplift during the Cretaceous, related to rifting in the Rockall Basin, with a kilometre-scale section of Jurassic stratigraphy removed. This part of the Erris Basin is dominated by a series of closely spaced (c. 1-2 km separation) westward-dipping faults in the Jurassic section (Fig. 9). Previous authors had interpreted these faults as through-going basement-linked structures (e.g. Shannon & Naylor, 1998; Chapman et al., 1999; Corfield et al., 1999). However more recent seismic profiles reveal their listric nature, with many faults detaching on the Uilleann Halite Member above

500 closely spaced salt rollers (e.g. Fig. 9). The Zechstein Group also acted as a décollement in
501 this part of the basin, mechanically detaching the Corrib Sandstone Formation from the
502 underlying Carboniferous basement. Salt pillows formed in the Zechstein Group and folded
503 the overlying Corrib Sandstone Formation in a similar manner to those in the Northern Slyne
504 Sub-basin (Fig. 5)

505 More faults are through-going across the Permian section in the Southern Erris Sub-basin
506 than in the Slyne Basin, suggesting that the Zechstein Group in this part of the basin may
507 contain a greater proportion of clastic lithologies. The proportion of salt decreases towards the
508 eastern margin of the Erris Basin, with faults being hard-linked through the Mesozoic and
509 Palaeozoic sections (Fig. 10). Only a thin layer of anhydrite was encountered in the 19/5-1
510 well drilled on the eastern edge of the Southern Erris Sub-basin (Fig. 4).

5.4. Northern Erris Sub-Basin

512 The Northern Erris Sub-basin is an asymmetric graben, bounded along its eastern margin by
513 the Irish Mainland Shelf, and separated from the Rockall Basin to the west by the narrow,
514 elongate Erris Ridge. The single well (12/13-1A) drilled in this part of the basin encountered
515 only sub-metre-scale stringers of anhydrite in a 19 m thick Zechstein Group section, while no
516 evaporite lithologies were present in the Currach or Meelagh formations. There is little
517 evidence on seismic sections to indicate the presence of significant thicknesses of salt in this
518 part of the basin, with all clearly imaged faults hard-linked through the Zechstein Group with
519 little evidence for growth sequences in the pre-Triassic sections (Fig. 11, 12).

520 There is similarly scarce evidence for salt in neighbouring areas; both wells in the Donegal
521 Basin to the northeast, 13/3-1 and 13/12-1 (Fig. 1), encountered the Pennsylvanian Blackthorn
522 Group directly beneath the Base-Cenozoic Unconformity (Texaco, 1978; Lundin, 2006), while
523 the 12/2-1 and 12/2-2 wells in the Rockall Basin to the west encountered the Triassic Cot
524 Sandstone Formation (lateral equivalent to the Corrib Sandstone Formation) and Upper
525 Jurassic Dawros Formation respectively lying directly above the Pennsylvanian Sorrel Group,
526 with no Permian, Upper Triassic or Lower Jurassic sediment encountered (Merlin Energy
527 Resources Consortium, 2020).

6. Discussion:

6.1.   Timing and drivers of halokinesis in the Slyne and Erris basins

Understanding the timing of salt movement during basin development is important both for unravelling the structural evolution and for understanding the development of the petroleum system. There is evidence of halokinesis occurring at several stages during basin evolution, including during both the Early to Middle Jurassic and Late Jurassic phases of rifting, in addition to post-rift modification of salt structures during the Cretaceous and Cenozoic.

In the Southern Slyne Sub-basin, the Triassic and Lower Jurassic section tilted above the large Zechstein Group salt roller is truncated by the Base Upper Jurassic unconformity (Fig. 7). This suggests that inflation of the salt roller in the footwall of the fault began forming during the Early-Middle Jurassic before the crest was eroded, resulting in the angular unconformity, followed by further inflation during Late Jurassic rifting (Fig. 13). In the Central Slyne Sub-basin growth sequences are observed in the Lower Jurassic section in the hanging walls of small intra-basinal listric faults which sole out in the Upper Permian Zechstein Group (Fig. 6). The faults controlling these growth sequences are then truncated by the Base Upper Jurassic Unconformity, indicating discrete extension confined to the Early-Middle Jurassic. There is further evidence of Early Jurassic halokinesis in the Northern Slyne Sub-basin with subtle thinning of the Lower Jurassic section onto the crest of the Corrib anticline (Fig. 5B), indicating that the Zechstein Group salt pillow was creating relief during the Early Jurassic (Fig. 13). Faults of a similar age are also interpreted in the Southern Erris Sub-basin, where faults which sole out above rollers of Uilleann Halite are truncated by the Base Upper Jurassic Unconformity. Several of these faults have hanging-wall sequences that record limited growth during the Early Jurassic (Fig. 9) and were reactivated during the main phase of rifting during the Late Jurassic and subsequently truncated by the Base-Cretaceous Unconformity.

The main phase of rifting in the Slyne and Erris basins, during the Late Jurassic, was preceded by the formation of the regional Base Upper Jurassic Unconformity mentioned previously (Fig. 13). The majority of intra-basinal faulting during this time occurred as thin-skinned, basement-detached deformation (Figs 5-7, 9) apart from in the Northern Erris Sub-basin where the Uilleann Halite Member is absent and the Zechstein Group is composed of carbonates and clastics (Fig. 11 & 12). In the Central Slyne Sub-basin growth sequences (Fig. 6A) and onlap (Fig. 6B) are observed on the flanks of the high-relief structures in the immediate hanging-wall of the basin-bounding fault. Unlike other high-relief structures where distinct crestal erosion is

561   recorded at the Base Upper Jurassic Unconformity, these structures likely emerged during

562   Late Jurassic basin extension (Fig. 13). Their geometry, as well as the likely presence of salt

563   in the Slyne Embayment to the west, indicate that these structures may have formed as forced

564   folds above the active footwall of the basin-bounding fault, creating the topography for onlap

565   and growth sequences (e.g. Withjack & Callaway, 2000; Coleman et al., 2017). The

566   interpretation of salt in the undrilled Slyne Embayment to the west of the Central Slyne Sub-

567   basin (Fig. 6A), further supports the idea that Permian salt and the overlying Mesozoic section

568   may have overstepped the now eroded footwall of the bounding fault before kilometre-scale

569   uplift and erosion during the Cretaceous and Cenozoic (Fig. 6A).

570   Along-strike variation in the anticlinal structures adjacent to the bounding fault in the Central

571   Slyne Sub-basin suggests there may be more complexity to their evolution beyond a breached

572   salt-detached monocline. Dancer et al. (1999) suggested five potential mechanisms for the

573   formation of the structure targeted by the 27/4-1 well (Fig. 6A), with one being salt diapirism.

574   Crucially, that paper predated the acquisition of good-quality 3D seismic data (2000) and the

575   drilling of the 27/4-1 well (2009), datasets which highlight the modification of these structures

576   during basin evolution. Specifically, the preservation of the Middle and Lower Jurassic section

577   proven in the 27/4-1 well, combined with the absence of the Kite Group and Dun Caan Shale

578   and Whitby Mudstone formations along-strike (Fig. 6C), highlights the modification of

579   structures during basin evolution, with the eroded crest of the structure in Fig. 6C being over

580   600ms TWT (c. 1200m) deeper than the seemingly uneroded crest of the structure in Fig. 6A.

581   This evidence suggests there may have been a high-relief salt-cored structure during the Early

582   and Middle Jurassic at the location of Fig. 6C, possibly a salt pillow or a large salt roller similar

583   to that imaged in Fig. 7 which exhibits comparable crestal erosion. This salt pillow or salt roller

584   collapsed during the Late Jurassic rifting with along-strike migration of the Permian salt into

585   the present-day higher elevation structures. As the apparent volume of salt present between

586   these anticlinal closures and the basin-bounding fault is relatively small, salt may also have

587   been extruded into salt diapirs on the now eroded footwall of the basin bounding fault.

588   Several salt structures in the Slyne Basin underwent significant post-rift modification during

589   the Cretaceous and Cenozoic, driven by rifting in the Rockall Basin during the Cretaceous,

590   and subsequent Cenozoic post-rift thermal subsidence, mid-Atlantic ridge-push and the

591   development of the Icelandic plume (Dancer et al., 1999). There is evidence throughout the

592   Slyne and Erris basins of fault reactivation, with several of these reactivations occurring in

593   salt-prone areas where the faults are listric and sole out in either the Zechstein Group or the

594   Uilleann Halite Member (Fig. 6 & 9). Other structures appear not to have been reactivated

595   during this post-rift activity (e.g. Fig. 7), although the lack of Cretaceous sediments in the

596   Central and Southern Slyne Sub-basins means that any fault movement during this phase of

597 post-rift deformation is not recorded. This Cretaceous and Cenozoic reactivation is subtle, with
598 movement on reactivated faults being in the order of 10s of metres, much lower than the syn-
599 rift fault offsets which are in the order of several hundred metres to kilometres in scale.

600 Regional extension is recognised as a common mechanism for the initiation of salt tectonics
601 (Jackson & Vendeville, 1994; Jackson & Hudec, 2017b) and is the most likely trigger for
602 halokinesis in the Slyne and Erris basins. The seismic data analysed above indicates that
603 there were two main phases of syn-rift halokinesis in the Slyne and Erris basins; the first of
604 these occurred during Early to Middle Jurassic extension with a subsequent phase of salt
605 movement during Late Jurassic rifting. Some salt structures formed during the first phase of
606 halokinesis were reactivated and continued to grow during the Late Jurassic period of salt
607 movement (e.g. Fig. 5-7), while others collapsed during this second phase of rifting (e.g. Fig.
608 6C). It is also possible that other structures such salt diapirs formed above the footwalls of
609 active faults due to extrusion of salt from collapsed structures which were subsequently eroded
610 during Cretaceous uplift. Several salt-related structures underwent minor modification during
611 post-rift tectonic activity in the Cretaceous and Cenozoic.

6.2.   Kinematic interaction between salt layers

613 In the Northern Slyne and Southern Erris sub-basins, two distinct layers of autochthonous salt
614 are present at different stratigraphic intervals, which has previously been termed 'double-
615 decker' salt tectonics (Corcoran & Mecklenburgh, 2005). In these areas a clear relationship
616 between the timing of halokinesis in each layer can be observed. The most well imaged of
617 these is the structure containing the Corrib gas field, where two discrete salt-related structures
618 are visible: a Zechstein Group salt pillow and an Uilleann Halite Member salt wall (Fig. 5B).
619 These structures have parallel trends, oriented NE-SW (Fig. 5D). The Uilleann Halite diapir
620 has a distinct pointed crest, indicating it is likely to be a reactive diapir which formed during
621 delamination faulting of the Jurassic overburden. As the Zechstein salt pillow grew and folded
622 the overlying Triassic and Jurassic section, outer-arc extension triggered listric delamination
623 faulting in the Jurassic section at the crest of the fold, with these faults soling out in the Uilleann
624 Halite (Fig. 13). The throw on these delamination faults is greatest at the apex of the Zechstein
625 salt pillow and resultant Lower Triassic fold, where outer-arc extension facilitates the inflation
626 of an Uilleann Halite salt roller (Fig. 5A) or in the case of the Corrib structure, a reactive diapir
627 oriented parallel to the fold axis of the salt pillow (Fig. 5B, D).

628 While the Zechstein salt pillow controlled the initial evolution of the Uilleann Halite diapir, the
629 subsequent growth of this diapir during continued extension may have in turn influenced the
630 development of the salt pillow. As regional extension continued during the Late Jurassic, the

631 delamination fault above the Corrib anticline experienced further normal movement. This fault
632 movement displaced the overburden section downwards off the crest of the anticline, creating
633 thicker sedimentary sections in the flanking synclines (Fig. 5B) while reducing the sediment
634 thickness at the apex of the fold. These thicker sedimentary sections on the flanks of the
635 anticline are suggested to have inflated the Zechstein salt pillow further through differential
636 loading, creating a steeper structure which would then lead to further movement on the crestal
637 delamination fault. The delamination fault above the Corrib gas field was reactivated again
638 during the Cretaceous and the Cenozoic, with distinct growth sequences observed in the
639 Cretaceous section in the immediate hanging-wall of the delamination fault (Fig. 5B), which
640 also offsets the top of the Druid Formation volcanics. This volcanic sequence is dated between
641 54.3 and 40 Ma (early-mid Eocene) in the 18/20-1 well and the 19/13-sb02 shallow borehole
642 in the Northern Slyne Sub-basin (Fugro, 1994; Corcoran & Mecklenburgh, 2005), indicating
643 how recently this Permian-Triassic salt relationship was active. A similar relationship likely
644 drove the syn- and post-rift evolution of other salt pillow and diapir pairs observed in the
645 Northern Slyne and Southern Erris sub-basins (e.g. Fig. 5A, 9).

646 Previous structural models for the Corrib structure (e.g. Corcoran & Mecklenburgh, 2005;
647 Dancer et al., 2005) have suggested a polarity reversal in the delamination fault at different
648 stages of basin evolution, with an initial westward-dipping fault plane during the Early Jurassic
649 changing to the dominant eastward-dipping fault observed today during the Late Jurassic. A
650 thinner Lower and Middle Jurassic section encountered on the eastern flank of the anticline
651 was interpreted as the eroded footwall of the westward-dipping fault relative to the thicker
652 section observed on the western flank (Fig. 5B). Recent biostratigraphic analysis has revealed
653 that complete Lias Group and Kite Group sections have been encountered in all wells drilled
654 in the Corrib gas field, with an attenuated but complete section encountered in the Lower and
655 Middle Jurassic on the eastern flank of the anticline (Merlin Energy Resources Consortium,
656 2020). This attenuated section was likely deposited on the crest of a salt-cored fold during the
657 Early and Middle Jurassic and is commonly observed above salt pillows (Jackson & Hudec,
658 2017a). Significant heave on the delamination fault during the Late Jurassic moved the
659 attenuated crestal section of Lower and Middle Jurassic sediments eastwards down the flank
660 of the anticline. It is therefore more likely that the delamination fault above the Corrib salt-
661 cored fold is a largely Late Jurassic structure which downthrows to the southeast. The polarity
662 reversal of faults above salt walls is a common feature of mature halokinetic structures (e.g.
663 Quirk & Pilcher, 2012) but due to the relative immaturity of the Upper Triassic salt wall a
664 simpler structural model prevails. Polarity reversal is observed in thickness variations in the
665 synclines flanking the Corrib anticline, with thicker Lower and Middle Jurassic section in the
666 NW syncline and a thicker Upper Jurassic section in the SE syncline. This reversal is likely a

667 result of the emergence of the kilometre-scale faults bounding the eastern margin of the
668 Northern Slyne Sub-basin during the Late Jurassic.

669 The kinematic interaction of stratigraphically discrete salt layers observed in the Slyne and
670 Erris basins may act as a structural template for other basins which have multiple thin layers
671 of salt (Fig. 13). Examples include the Sole Pit Basin and Danish Central Graben in the North
672 Sea, where delamination faults sole out in the Triassic Muschelkalk Halite above folds cored
673 by Zechstein Group salt (Glennie, 1997; Hansen et al., 2020).

6.3.   Relationship between timing of halokinesis and the petroleum system

676 The timing of formation and subsequent modification of the Corrib structure played a crucial
677 role in both the success and failure of the 18/20-1 discovery well. The well was drilled to the
678 northwest of the main delamination fault, passing through the tilted fault block above the
679 Uilleann Halite diapir (Fig. 5B, D). The well encountered oil-stained sandstones throughout
680 the Upper Jurassic section, evidence of a breached paleo-accumulation, before discovering
681 the gas accumulation in the Corrib Sandstone Formation, sealed by the Uilleann Halite
682 Member (Enterprise, 1996b; Dancer et al., 2005). Geochemical fingerprinting of these
683 hydrocarbon fluids indicates that the oil is sourced from the Lower Jurassic Whitby Mudstone,
684 Pabay Shale and Dun Caan Shale formations while the gas is presumed to be generated by
685 coal layers in the Carboniferous basement (Dancer et al., 1999; Scotchman et al., 2018). Post-
686 rift movement on the main delamination fault bounding the Jurassic structural trap (Fig. 5D)
687 during both the Cretaceous (Fig. 5D) and Cenozoic (Fig. 5B) post-dates the main phase of
688 hydrocarbon generation and migration at the end of the Jurassic (Petroleum Affairs Division,
689 2005). This late movement on the delamination fault likely caused cross-fault juxtaposition of
690 Upper Jurassic sandstones, possible dilation of the fault plane and breaching of the top seal,
691 leading to the loss of the oil accumulation. However, since the delamination fault soles out in
692 the Uilleann Halite Member, this post-charge fault movement did not interact with the Corrib
693 Sandstone Formation and the gas accumulation.

694 Similarly, post-rift modification of the underlying Zechstein Group salt pillow may explain the
695 nature of the Corrib anticlinal trap. The anticline is significantly underfilled, with potential
696 associated mechanisms including the presence of a small leaking fault at the current gas-
697 water contact or leakage through the sealing Uilleann Halite Member during Cretaceous and
698 Cenozoic exhumation (Corcoran & Doré, 2002; Corcoran & Mecklenburgh, 2005). The modest
699 overpressure within the reservoir section (Corcoran & Doré, 2002) and halite composition of
700 the top-seal indicate that the original charge pre-dating exhumation is preserved and that

701   leakage without clear evidence of salt-welding is difficult. Salt tectonics may instead be
702   responsible for the underfilled nature of the Corrib anticline, with post-rift movement on the
703   delamination fault and growth of the Uilleann Halite Member diapir perhaps driven by post-rift
704   growth of the Zechstein Group salt pillow. Additional post-rift (and post-charge) growth of this
705   salt pillow would have increased the vertical relief of the anticline and its trap capacity. The
706   volume of the structural trap from the Late Cretaceous onwards would therefore be larger than
707   the volume of gas trapped during the Late Jurassic and Early Cretaceous, resulting in its
708   underfilled nature observed at present. This highlights the multiphase evolution of this and
709   probably other structures within the Slyne and Erris basins and illustrates how understanding
710   their structural history will be critical to improving exploration success in the future.

6.4. The Slyne and Erris basins in context with other salt-prone basins of the North Atlantic

Results presented thus far have highlighted the importance of salt during the structural evolution of the Slyne and Erris basins and defined a range of structures that are characteristic of salt-involved deformation in this area. By applying a similar methodology to that demonstrated above, we can delimit the occurrence of salt in neighbouring basins where the lack of well data has made interpretation of salt more speculative. A more detailed understanding of salt distribution can in turn be used to refine paleogeographic models for the Late Permian and Late Triassic of the Irish Atlantic margin.

6.4.1. Irish Atlantic Margin

No Permian rocks have been encountered outside of the Slyne and Erris basins on the Irish Atlantic margin to date, although Permian ages have been suggested for a sandstone section encountered above the Carboniferous in the 12/2-1 and 12/2-2 wells on the eastern margin of the Rockall Basin, adjacent to the northern Erris Basin (Shell, 2009; Tyrrell et al., 2010). Conversely, Early and Late Triassic-aged sections have been proven in several basins, including the Porcupine and Celtic Sea basins.

In the North Porcupine Basin metre-scale anhydrite layers were encountered towards the top of the Currach Formation in well 26/22-1A (BP, 1979), while the 35/19-1A well encountered 24m of allochthonous salt in Upper Jurassic sediments on the eastern margin of the Porcupine Basin (Britoil, 1986). In this well the salt is composed of massive halite with thin slivers of red mudstone likely representing rafted sections of Currach Formation mudstones, suggestive of Upper Triassic salt, equivalent to the Uilleann Halite Member in the Slyne and Erris basins. As an Uilleann Halite Member equivalent has not been encountered in the northern Porcupine Basin to date, this Triassic salt is likely to have migrated from a more central, undrilled part of the basin to the south.

The Goban Spur Basin, along the southern margin of the Porcupine Basin (Fig. 1), may also contain Triassic salt, with evidence on seismic data of décollement surfaces and salt pillows beneath the Base-Cretaceous Unconformity (Fig. 14). A pronounced fold occurring above near-horizontal, unfolded reflectors (Fig. 14) is interpreted as local Lower Triassic sediments deposited within the Variscan fold and thrust belt but since the single well drilled in the Goban Spur Basin terminated in Lower Jurassic sediments, this interpretation remains speculation (Colin et al., 1992).

743 Previous authors have noted décollement surfaces in the perched basins along the margins
744 of the Irish sector of the Rockall Basin, including the Bróna and Fursa basins on the eastern
745 margin (Thomson & McWilliam, 2001; Štolfová & Shannon, 2009) and the Conall and Rónán
746 basins on the north-western margin (Corfield et al., 1999; Walsh et al., 1999). Distinct
747 detachment horizons are visible on seismic data from these basins, with faults observed soling
748 out in these horizons. In the Rónán Basin on the western margin of the Rockall Basin, a subtle
749 décollement is visible within the steeply dipping reflectors, mechanically detaching faults
750 above and below it, with a distinct local thickening along the south-eastern margin of the basin
751 interpreted as a salt pillow (Fig. 15A). Similarly, two distinct sets of faults are observed either
752 side of a décollement in the Fursa Basin (Fig. 15B). While these basins are undrilled at
753 present, these décollement surfaces likely represent lateral equivalents to Permian salt proven
754 in the Slyne Basin, as interpreted by Štolfová & Shannon (2009). In these basins this layer of
755 salt plays a similar role in mechanically detaching the Mesozoic basin fill, which displays
756 similar seismic facies to those observed in the Slyne and Erris basins, from the Palaeozoic
757 basement.

758 ## 6.4.2.   Neighbouring basins on the European Atlantic
759 margin

760 The basins of the Irish Atlantic margin belong to a chain of basins that extend along the
761 European Atlantic margin, many of which also contain significant salt deposits that correlate
762 with those proven in the Slyne and Erris basins. Directly north of the study area, a series of
763 interconnected basins off the north-western coast of the UK contain significant thicknesses of
764 sediments defined broadly as Permo-Triassic due to the relative lack of biostratigraphic control
765 (Steel & Wilson, 1975; Hitchen et al., 1995). Both wells drilled in the West Orkney Basin
766 encountered several hundred metres of halite interbedded with sandstones and mudstones
767 with anhydrite stringers belonging to the West Orkeny Evaporite Formation interpreted as
768 being Permian in age and representing Zechstein Group equivalents (Elf, 1991; Hitchen et al.,
769 1995; McKie, 2017). Along-strike in the West Shetland Basin the 205/27a-1 well encountered
770 interbedded Upper Permian sandstones and mudstones with anhydrite stringers (Hitchen et
771 al., 1995). There is little evidence of salt in the Upper Triassic section in this region, instead
772 being dominated by sandstone (Swiecicki *et al.* 1995).

6.4.3.   Implications for the Permian & Triassic paleogeography of the Irish Atlantic margin

Paleogeographic reconstructions of north-western Europe during the Permian and Triassic often present the Irish Atlantic margin in simplified terms at the fringes of regional maps, owing to the relative lack of well penetrations and published data when compared with neighbouring regions. The Early Triassic is an exception, due to its significance in the petroleum system of the Corrib gas field (Dancer et al., 2005), with a relatively well understood paleogeography in which the Slyne and Erris basins are host to southwards-verging braided fluvial systems (e.g. Tyrell et al., 2007; McKie & Williams, 2009; Franklin et al., 2019). No Early Permian rocks have been encountered on the Irish Atlantic margin to date. Existing paleogeographic reconstructions (e.g. Doré, 1991; Knott et al., 1993; McKie & Shannon, 2011; McKie, 2017; Scotese & Schettino, 2017) present the Irish Atlantic margin as the terminus of tortuous seaways that extended into the Pangean supercontinent; During the Late Permian ingress of marine waters came from the Boreal Ocean to the north through the West of Shetland region, but during the Late Triassic a seaway extended from the Tethys Ocean to the southeast across Central and Western Europe to reach Ireland through the Cheshire Basin in the UK. Using the results presented in this study as well as the speculative interpretations of neighbouring regions discussed above, it is possible to refine existing paleogeographic models of the region during the Late Permian and Late Triassic, and include the basin-specific detail for the Irish Atlantic margin that was absent in previous regional syntheses.

The distribution of Late Permian salt of both the UK and Norwegian North Sea has been interpreted to be fault controlled, with salt-prone lithologies deposited in the hanging walls of active faults, while marginal carbonate and siliciclastic facies accumulated on basin margins and intra-basinal highs. The exact age of faulting remains ambiguous, with the Late Permian bathymetry either being inherited from Early Permian rifting, or representing syn-depositional extension in the Late Permian (e.g. McKie & Shannon, 2011; Jackson & Lewis, 2016; Jackson et al., 2019). Applying a similar model to the Slyne and Erris basins, the thicker salt-prone Zechstein Group in the Slyne Basin and the Southern Erris Sub-basin would be indicative of active Permian faulting, while the presence of thin marginal deposits in the Northern Erris Sub-basin suggests this area was a relative high with little active faulting. Therefore, the marine pathway connecting the Slyne Basin to the Boreal Ocean likely traversed an area other than the Erris Basin, an interpretation supported by the lack of Permian sediments in the north-eastern Irish Rockall Basin, the Donegal Basin and the Sea of the Hebrides Basin. The layers of salt interpreted in the Rónán Basin, the pre-Cretaceous 'conjugate margin' to the Erris Basin (Fig. 15A), might therefore indicate that the route of active Permian rifting may have been an

808   anastomosing series of rifts extending northwards along the axis of a proto-Rockall and West
809   of Shetland rift system, with remnants of these basins occupying the margins of the Rockall
810   Basin after rifting and hyperextension in the Cretaceous (Fig. 16A). This may indicate that the
811   framework for the present-day configuration of rift basins on the Irish Atlantic margin may have
812   been established in-part during this period of Permian extension.

813   During the Late Triassic, the Northern Slyne and Southern Erris sub-basins may have also
814   been the terminus for a seaway, this time stretching from the Tethys Ocean to the southwest.
815   The Uilleann Halite Member in the Northern Slyne and Southern Erris sub-basins (Fig. 1, 8)
816   likely represents the deposits of incursions of marine brines from the southwest. In
817   neighbouring regions such as the Ulster Basin and the Irish Sea basins several discrete layers
818   of halite are interpreted as successive marine flooding events into these regions (Jackson &
819   Mulholland, 1993; Dunford et al., 2001; McKie, 2017). The Uilleann Halite Member might
820   therefore represent the deposits of a more extensive marine incursion that extended beyond
821   those found in the Irish Sea and North Channel region. The exact route of marine ingress is
822   uncertain and likely obscured by Cretaceous and Cenozoic erosion, but may have come from
823   the south, through the Celtic Sea and Porcupine basins (e.g. Scotese & Schettino, 2017), or
824   from the north or east through the Donegal Basin or the Ulster-Larne Basin (e.g. Naylor, 1992).
825   The paleogeography of the Late Triassic salt layers is distinct from the Late Permian as these
826   marine incursions flood a predominantly arid lacustrine environment, represented by the thick
827   red mudstones which dominate the majority of the Currach Formation (Fig. 8), which differs
828   from the predominantly marine environment of the Zechstein Group deposits, represented by
829   cleaner halite with few mudstone inclusions (Fig. 4). Additionally, the Triassic was a period of
830   tectonic quiescence on the Irish Atlantic margin following Permian rifting (e.g. Tyrrell et al.,
831   2007; Franklin et al., 2019) and Late Triassic sediments likely spilled out beyond the present-
832   day basin boundaries (Fig. 16B), with their present-day distribution a product of preservation
833   in post-Triassic rift basins.

7. Conclusions

Using a combination of 2D and 3D seismic, wireline, and core data, this study investigated the distribution of the salt in the Slyne and Erris basins and its influence on the structural evolution of these basins.

1. Two main salt-prone intervals are present in the Slyne and Erris basins. The Upper Permian Zechstein Group is salt prone throughout the Slyne Basin and in the Southern Erris Sub-basin, becoming dominated by carbonates and clastics in the Northern Erris Sub-basin. The Upper Triassic Uilleann Halite Member is developed in the Northern Slyne Basin and Southern Erris sub-basins.

2. Salt acts as a décollement and mechanically detaches distinct sections of stratigraphy within the Slyne and Erris basins. The Zechstein Group has the largest impact on basin development and is a regional décollement surface, with most syn-rift normal faults detached from the pre-Permian basement along this surface. The Uilleann Halite Member exerts similar controls on basin development where it is present.

3. Halokinesis occurred at several stages during the evolution of the Slyne and Erris basins. This includes extension in the Early Jurassic and the Late Jurassic, as well as post-rift reactivation during the Cretaceous and Cenozoic. This salt movement has created a variety of relatively immature salt-related structures throughout the Slyne and Erris basins, including salt pillows, rollers and reactive diapirs.

4. Where both salt successions are developed, the topography created by the Zechstein Group halokinesis influences the development of salt-related structures in the overlying Uilleann Halite Member, exemplified in the parallel salt pillow and salt wall pair observed in the Corrib structure. Outer-arc extension and gravitational collapse linked with the formation of the Zechstein Group salt pillows leads to the formation of Uilleann Halite salt rollers and walls. This kinematic interaction may serve as a framework for the structural evolution of similar structures in other basins with multiple stratigraphically discrete layers of salt.

5. An improved understanding of the distribution and composition of Permian and Triassic salt in the Slyne and Erris basins and in undrilled basins along the Irish Atlantic margin indicates that the framework of sedimentary basins along the Irish Atlantic margin may have been established as early as the Late Permian.

References

Alves, T.M., Moita, C., Sandnes, F., Cunha, T., Monteiro, J.H. & Pinheiro, L.M. 2006. Mesozoic-Cenozoic evolution of North Atlantic continental-slope basins: The Peniche basin, western Iberian margin. *AAPG Bulletin*, **90**, 31–60.

Ambassador 1962. Dowra No. 1 Well Report. Ambassador Irish Oil Company.

Amoco 1978. Well 19/5-1 Geological Completion Report. Amoco Ireland Exploration Company, compiled by Odell, R.T. & Thomas, I.W.

Amoco 1979. Wells 12/13-1 and 12/13-1A Geological Completion Report. Amoco Ireland Exploration Company, compiled by Odell, R.T. & Walker, D.

Anderson, H., Walsh, J.J. & Cooper, M.R. 2018. The development of a regional-scale intraplate strike-slip fault system; Alpine deformation in the north of Ireland. *Journal of Structural Geology*, **116**, 47–63.

Biancotto, F., Hardy, R.J.J., Jones, S.M., Brennan, D. & White, N.J. 2007. Estimating denudation from seismic velocities offshore NW Ireland. *Society of Exploration Geophysicists - 77th SEG International Exposition and Annual Meeting, SEG 2007*, 407–411.

BP 1979. Ireland, Porcupine Basin Well 26/22-1A Geological Completion Report. BP Petroleum Development Ltd. (Irish Branch), compiled by Dryden, G.J.

Britoil 1986. Eire Licence 1/82 evaluation of well 35/19-1. Britoil plc, compiled by Harvey, M. A. & Wild, J. L.

Brown, A.R. 2001. Calibrate yourself to your data! A vital first step in seismic interpretation. *Geophysical Prospecting*, **49**, 729–733.

Brown, A.R. 2011. *Interpretation of Three-Dimensional Seismic Data*. Society of Exploration Geophysicists & American Association of Petroleum Geologists.

Chapman, T.J. 1989. The Permian to Cretaceous structural evolution of the Western Approaches Basin (Melville sub-basin), UK. *Geological Society, London, Special Publications*, **44**, 177–200.

Chapman, T.J., Broks, T.M., Corcoran, D.V., Duncan, L.A. & Dancer, P.N. 1999. The structural evolution of the Erris Trough, offshore northwest Ireland , and implications for hydrocarbon generation. *Petroleum Geology of Northwest Europe: Proceedings of the 5th Conference*, 455–469.

Chew, D.M. & Stillman, C.J. 2009. Late Caledonian orogeny and magmatism. *In*: *The Geology of Ireland*. 143–173.

Coleman, A.J., Jackson, C.A.L. & Duffy, O.B. 2017. Balancing sub- and supra-salt strain in salt-influenced rifts: Implications for extension estimates. *Journal of Structural Geology*, **102**, 208–225.

901   Colin, J.-P., Ioannides, N.S. & Vining, B. 1992. Mesozoic stratigraphy of the Goban Spur,
902   offshore south-west Ireland. *Marine and Petroleum Geology*, **9**, 527–541.

903   Cooper, M.R., Anderson, H., Walsh, J.J., Van Dam, C.L., Young, M.E., Earls, G. & Walker,
904   A. 2012. Palaeogene Alpine tectonics and Icelandic plume-related magmatism and
905   deformation in Northern Ireland. *Journal of the Geological Society*, **169**, 29–36.

906   Corcoran, D. V & Doré, A.G. 2002. Depressurization of hydrocarbon-bearing reservoirs in
907   exhumed basin settings: evidence from Atlantic margin and borderland basins.
908   *Exhumation of the North Atlantic Margin: Timing, Mechanisms and Implications for*
909   *Petroleum Exploration*, **196**, 457–483.

910   Corcoran, D. V & Mecklenburgh, R. 2005. Exhumation of the Corrib Gas Field, Slyne Basin,
911   offshore Ireland. *Petroleum Geoscience*, **11**, 239–256.

912   Corfield, S., Murphy, N. & Parker, S. 1999. The structural and stratigraphic framework of the
913   Irish Rockall Trough. *Geological Society, London, Petroleum Geology Conference*
914   *series*, **5**, 407–420.

915   Coward, M.P. 1995. Structural and tectonic setting of the Permo-Triassic basins of northwest
916   Europe. *Geological Society, London, Special Publications*, **91**, 7–39.

917   Cunningham, G.A. & Shannon, P.M. 1997. The Erris Ridge: A major geological feature in the
918   NW Irish Offshore Basins. *Journal of the Geological Society*, **154**, 503–508.

919   Croker, P.F. and Shannon, P.M. 1987. The evolution and hydrocarbon prospectivity of the
920   Porcupine Basin, Offshore Ireland. *Petroleum Geology of Northwest Europe*, **3**, 633–
921   642.

922   Dancer, P.N., Algar, S.T. & Wilson, I.R. 1999. Structural evolution of the Slyne Trough.
923   *Petroleum Geology of Northwest Europe: Proceedings of the 5th Conference on the*
924   *Petroleum Geology of Northwest Europe*, **1**, 445–454.

925   Dancer, P.N. & Pillar, N.W. 2001. Exploring in the Slyne Basin: a geophysical challenge. *The*
926   *Petroleum Exploration of Ireland's Offshore Basins*, **188**, 209–222.

927   Dancer, P.N., Kenyon-Roberts, S.M., Downey, J.W., Baillie, J.M., Meadows, N.S. & Maguire,
928   K. 2005. The Corrib gas field, offshore west of Ireland. *Geological Society, London,*
929   *Petroleum Geology Conference series*, **6**, 1035–1046.

930   Deptuck, M.E. & Kendell, K.L. 2017. A Review of Mesozoic-Cenozoic Salt Tectonics Along
931   the Scotian Margin, Eastern Canada. *In*: *Permo-Triassic Salt Provinces of Europe,*
932   *North Africa and the Atlantic Margins*. Elsevier, 287–312.

933   Doré, A. 1991. The structural foundation and evolution of Mesozoic seaways between
934   Europe and the Arctic. *Palaeogeography, Palaeoclimatology, Palaeoecology*, **87**, 441–
935   492.

936   Doré, A.G., Lundin, E.R., Jensen, L.N., Birkeland, O., Eliassen, P.E. & Fichler, C. 1999.
937   Principal tectonic events in the evolution of the northwest European Atlantic margin.
938   *Petroleum Geology of Northwest Europe: Proceedings of the 5th Conference*, 41–61.

939 Duffy, O.B., Gawthorpe, R.L., Docherty, M. & Brocklehurst, S.H. 2013. Mobile evaporite
940   controls on the structural style and evolution of rift basins: Danish Central Graben,
941   North Sea. *Basin Research*, **25**, 310–330.

942 Dunford, G.M., Dancer, P.N. & Long, K.D. 2001. Hydrocarbon potential of the Kish Bank
943   Basin: integration within a regional model for the Greater Irish Sea Basin. *Geological*
944   *Society, London, Special Publications*, **188**, 135–154.

945 Elf 1991. Final Well Report 202/18-1. Elf Enterprise Caledonia Ltd.

946 Enterprise 1996a. Well IRE 27/5-1 Geological Completion Report. Enterprise Oil plc,
947   compiled by Rawlinson, A., Verlander, J., Scotchman, I. & Henderson, G.

948 Enterprise 1996b. IRE 18/20-1 Geological Completion Report. Enterprise Oil plc, compiled
949   by O'Neill, N., Scotchman, I. & Dancer, N.

950 Enterprise 2000a. Well IRE 18/25-2 Geological Completion Report. Enterprise Oil plc,
951   compiled by Pay, M. & Geerlings, P.

952 Enterprise 2000b. Well IRE 18/20-3 Geological Completion Report. Enterprise Oil plc,
953   compiled by Pay, M. & Geerlings, P.

954 Enterprise 2000c. Well IRE 18/20-4 Geological Completion Report. Enterprise Oil plc,
955   compiled by Pay, M. & Geerlings, P.

956 Ferrer, O., Jackson, M.P.A., Roca, E. & Rubinat, M. 2012. Evolution of salt structures during
957   extension and inversion of the Offshore Parentis Basin (Eastern Bay of Biscay).
958   *Geological Society Special Publication*, **363**, 361–380.

959 Franklin, J., Tyrrell, S., Morton, A., Frei, D. & Mark, C. 2019. Triassic sand supply to the
960   Slyne Basin, offshore western Ireland – new insights from a multi-proxy provenance
961   approach. *Journal of the Geological Society*, **176**, 1120–1135.

962 Fugro. 1994. Field Report Irish Frontier Shallow Coring Project Blocks 19/13 and 27/24 Irish
963   Sector Atlantic Ocean (Volume I).

964 Gardiner, P.R.R. & Visscher, H. 1971. Permian–Triassic Transition Sequence at Kingscourt,
965   Ireland. *Nature Physical Science*, **229**, 209–210.

966 Gardiner, P.R.R. & McArdle, P. 1992. The geological setting of Permian gypsum and
967   anhydrite deposits in the Kingscourt district, counties Cavan, Meath and Monaghan.
968   *The Irish minerals industry*, 1980 – *1990,* 301-316

969 Gerlings, J., Hopper, J.R., Fyhn, M.B.W. & Frandsen, N. 2017. Mesozoic and older rift
970   basins on the SE Greenland Shelf offshore Ammassalik. *Geological Society Special*
971   *Publication*, **447**, 375–392.

972 Glennie, K.W., 1997. History of exploration in the southern North Sea. *Geological Society,*
973   *London, Special Publications*, **123**, 5-16.

974 Grennan, E. 1992. The Glangevlin gypsum deposit, Co. Cavan. *The Irish minerals*
975   *industry*, 1980 - *1990*, 317-325.

976   Hansen, T. H., Clausen, O. R., & Andresen, K. J. (in review) 2020. Thick- and thin-skinned
977   basin inversion in the Danish Central Graben, North Sea – the role of deep evaporites
978   and basement kinematics. *Solid Earth Discuss.* https://doi.org/10.5194/se-2020-127

979   Haughton, P., Praeg, D., Shannon, P., Harrington, G., Higgs, K., Amy, L., Tyrrell, S. &
980   Morrissey, T. 2005. First results from shallow stratigraphic boreholes on the eastern
981   flank of the Rockall Basin, offshore western Ireland. *Geological Society, London,*
982   *Petroleum Geology Conference series*, **6**, 1077–1094.

983   Hitchen, K., Stoker, M.S., Evans, D. & Beddoe-Stephens, B. 1995. Permo-Triassic
984   sedimentary and volcanic rocks in basins to the north and west of Scotland. *Geological*
985   *Society, London, Special Publications*, **91**, 87–102.

986   Hudec, M.R. & Jackson, M.P.A. 2007. Terra infirma: Understanding salt tectonics. *Earth-*
987   *Science Reviews*, **82**, 1–28.

988   Hutton, D.H.W. & Alsop, G.I. 1996. The Caledonian strike-swing and associated lineaments
989   in NW Ireland and adjacent areas: sedimentation, deformation and igneous intrusion
990   patterns. *Journal of the Geological Society*, **153**, 345–360.

991   Illing, L. V & Griffith, A.E. 1986. Gas Prospects in the 'Midland Valley' of Northern Ireland.
992   *Geological Society, London, Special Publications*, **23**, 73–84.

993   Jackson, C.A.L. & Lewis, M.M. 2016. Structural style and evolution of a salt-influenced rift
994   basin margin; the impact of variations in salt composition and the role of polyphase
995   extension. *Basin Research*, **28**, 81–102.

996   Jackson, C.A.-L. & Stewart, S.A. 2017. Composition, Tectonics, and Hydrocarbon
997   Significance of Zechstein Supergroup Salt on the United Kingdom and Norwegian
998   Continental Shelves. *In*: *Permo-Triassic Salt Provinces of Europe, North Africa and the*
999   *Atlantic Margins*. Elsevier, 175–201.

1000   Jackson, C.A.L., Elliott, G.M., Royce-Rogers, E., Gawthorpe, R.L. & Aas, T.E. 2019. Salt
1001   thickness and composition influence rift structural style, northern North Sea, offshore
1002   Norway. *Basin Research*, **31**, 514–538.

1003   Jackson, D.I. & Mulholland, P. 1993. Tectonic and stratigraphic aspects of the East Irish Sea
1004   Basin and adjacent areas: contrasts in their post-Carboniferous structural styles.
1005   *Geological Society, London, Petroleum Geology Conference series*, **4**, 791–808.

1006   Jackson, M.P.A. & Vendeville, B.C. 1994. Regional extension as a geologic trigger for
1007   diapirism. *Geological Society of America Bulletin*, **106**, 57–73.

1008   Jackson, M.P., & Hudec, M.R. 2017a. *Salt tectonics: Principles and practice*. Cambridge
1009   University Press. 62-75.

1010   Jackson, M.P., & Hudec, M.R. 2017b. *Salt tectonics: Principles and practice*. Cambridge
1011   University Press. 256-303.

1012   Jansa, L.F., Bujak, J.P. & Williams, G.L. 1980. Upper Triassic salt deposits of the western
1013   North Atlantic. *Canadian Journal of Earth Sciences*, **17**, 547–559.

Jolley, D.W. & Bell, B.R. 2002. The evolution of the North Atlantic Igneous Province and the opening of the NE Atlantic rift. *Geological Society, London, Special Publications*, **197**, 1–13.

Knott, S.D., Burchell, M.T., Jolley, E.J. & Fraser, A.J. 1993. Mesozoic to Cenozoic plate reconstructions of the North Atlantic and hydrocarbon plays of the Atlantic margins. *Petroleum Geology of Northwest Europe: Proceedings of the 4th Conference*, 953–974.

Le Breton, E., Cobbold, P.R. & Zanella, A. 2013. Cenozoic reactivation of the Great Glen Fault, Scotland: additional evidence and possible causes. *Journal of the Geological Society*, **170**, 403–415.

Lundin 2006. Well 13/12-1 Inishbeg Prospect End of Well Report. Lundin Britain Ltd., compiled by Craig, D. & Welding, P.

McCann, N. 1988. An Assessment of the Subsurface Geology between Magilligan Point and Fair Head, Northern Ireland. *Irish Journal of Earth Sciences*, **9**, 71–78.

McKie, T. & Shannon, P.M. 2011. Comment on 'The Permian-Triassic transition and the onset of Mesozoic sedimentation at the northwestern peri Tethyan domain scale: Palaeogeographic maps and geodynamic implications' by S. Bourquin, A. Bercovici, J. López-Gomez, J. B. Diez, J. Broutin, A. . *Palaeogeography, Palaeoclimatology, Palaeoecology*, **311**, 136–143.

McKie, T. 2017. Paleogeographic Evolution of Latest Permian and Triassic Salt Basins in Northwest Europe. *In*: *Permo-Triassic Salt Provinces of Europe, North Africa and the Atlantic Margins*. Elsevier, 159–173.

Merlin Energy Resources Consortium. 2020. The Standard Stratigraphic Nomenclature of Offshore Ireland: An Integrated Lithostratigraphic, Biostratigraphic and Sequence Stratigraphic Framework. Project Atlas. Petroleum Affairs Division, Department of the Environment, Climate and Communications, Special Publication **1/21**.

Naylor, D. & Shannon, P., 1982. Geology of offshore Ireland and west Britain.

Naylor, D., Shannon, P.M. and Murphy, N. 1999. *Irish Rockall Basin Region - a Standard Structural Nomenclature System*. Petroleum Affairs Division, Department of the Environment, Climate and Communications, Special Publication **1/99**.

Naylor, D. 1992. The post-Variscan history of Ireland. *Geological Society, London, Special Publications*, **62**, 255–275, https://doi.org/10.1144/GSL.SP.1992.062.01.21.

Naylor, D., Haughey, N., Clayton, G. & Graham, J.R. 1993. The Kish Bank Basin, offshore Ireland. *Petroleum Geology of Northwest Europe: Proceedings of the 4th Conference*, **4**, 845–855, https://doi.org/10.1144/0040845.

Pena dos Reis, R., Pimentel, N., Fainstein, R., Reis, M. & Rasmussen, B. 2017. Influence of Salt Diapirism on the Basin Architecture and Hydrocarbon Prospects of the Western Iberian Margin. *In*: *Permo-Triassic Salt Provinces of Europe, North Africa and the Atlantic Margins*. Elsevier, 313–329.

1052 Petroleum Affairs Division. 2005. *Petroleum Systems Analysis of the Slyne, Erris and*
1053   *Donegal Basins Offshore Ireland - Digital Atlas*. Petroleum Affairs Division, Department
1054   of the Environment, Climate and Communications, Special Publications **1/05**.

1055 Quinn, M.F., Smith, K. & Bulat, J. 2010. A Geological Interpretation of the Nearshore Area
1056   between Belfast Lough and Cushendun, Northern Ireland, Utilising a Newly Acquired
1057   2D Seismic Dataset to Explore for Salt Layers for Possible Gas Storage within Man-
1058   Made Caverns. *British Geological Survey Commissioned Report CR/10/069*.

1059 Raine, R., Copestake, P., Simms, M.J. & Boomer, I. 2020. Uppermost Triassic to Lower
1060   Jurassic sediments of the island of Ireland and its surrounding basins. *Proceedings of*
1061   *the Geologists' Association*.

1062 Ramos, A., Fernández, O., Muñoz, J.A. & Terrinha, P. 2017. Impact of basin structure and
1063   evaporite distribution on salt tectonics in the Algarve Basin, Southwest Iberian margin.
1064   *Marine and Petroleum Geology*, **88**, 961–984.

1065 Robinson, K.W., Shannon, P.M. & Young, D.G.G. 1981. The Fastnet Basin: An Integrated
1066   Analysis. *In*: Illing, L. V. and Hobson, G. D. (eds) *Petroleum Geology of the Continental*
1067   *Shelf of North-West Europe*.

1068 Rojo, L.A., Cardozo, N., Escalona, A. & Koyi, H. 2019. Structural style and evolution of the
1069   Nordkapp Basin, Norwegian Barents Sea. *AAPG Bulletin*, **103**, 2177–2217.

1070 Schiffer, C., Doré, A.G., Foulger, G.R., Franke, D., Geoffroy, L., Gernigon, L., Holdsworth,
1071   R.E., Kusznir, N., Lundin, E., McCaffrey, K., Peace, A.L., Petersen, K.D., Phillips, T.B.,
1072   Stephenson, R., Stoker, M.S. & Welford J.K. 2019. Structural inheritance in the North
1073   Atlantic. *Earth-Science Reviews*, 102975.

1074 Scotchman, I.C., Doré, A.G. & Spencer, A.M. 2018. Petroleum systems and results of
1075   exploration on the Atlantic margins of the UK, Faroes & Ireland: what have we
1076   learnt? *Geological Society, London, Petroleum Geology Conference series*, **8**, 187–
1077   197, https://doi.org/10.1144/PGC8.14.

1078 Scotese, C.R. & Schettino, A. 2017. Late Permian-Early Jurassic Paleogeography of
1079   Western Tethys and the World. *In*: *Permo-Triassic Salt Provinces of Europe, North*
1080   *Africa and the Atlantic Margins*. Elsevier, 57–95.

1081 Shannon, P.M. 1991. Tectonic framework and petroleum potential of the Celtic Sea, Ireland.
1082   *First Break*, **9**, https://doi.org/10.3997/1365-2397.1991006.

1083 Shannon, P.M. & Naylor, D. 1998. An assessment of Irish offshore basins and petroleum
1084   plays. *Journal of Petroleum Geology*, **21**, 125–152.

1085 Shell 2009. IRE 12/2-1 West Dooish Exploration Well End of Well Report – Volume 2
1086   Subsurface Section. Shell E&P Ireland Ltd.

1087 Statoil 2004. Well 19/11-1 & 1A Final Well Report. Statoil Exploration (Ireland) Ltd., compiled
1088   by Hofsøy, R., Skagen, J., Mortensen, H. & Conroy, J.

1089 StatoilHydro 2009. Well 19/8-1 Cashel Prospect End of Well Report. Statoil Exploration
1090   (Ireland) Ltd., compiled by MacTiernan, B., Kleppa, S., Hunnes, O., Sigve-Selnes, K. &
1091   Igbineweka, O.J.

1092 Stewart, S.A., Harvey, M.J., Otto, S.C. & Weston, P.J. 1996. Influence of salt on fault
1093   geometry: examples from the UK salt basins. *Geological Society, London, Special*
1094   *Publications*, **100**, 175–202.

1095 Stewart, S.A. 2007. Salt tectonics in the North Sea Basin: a structural style template for
1096   seismic interpreters. *Geological Society, London, Special Publications*, **272**, 361–396.

1097 Stoker, M.S., Stewart, M.A., Shannon, P.M., Bjerager, M., Nielsen, T., Blischke, A.,
1098   Hjelstuen, B.O., Gaina, C., McDermott, K. & Ólavsdóttir, J. 2017. An overview of the
1099   Upper Palaeozoic–Mesozoic stratigraphy of the NE Atlantic region. *Geological Society,*
1100   *London, Special Publications*, **447**, 11–68, https://doi.org/10.1144/SP447.2.

1101 Štolfová, K. & Shannon, P.M. 2009. Permo-Triassic development from Ireland to Norway:
1102   basin architecture and regional controls. *Geological Journal*, **44**, 652–676.

1103 Steel, R.J. & Wilson, A.C. 1975. Sedimentation and tectonism (?Permo-Triassic) on the
1104   margin of the North Minch Basin. *Journal of the Geological Society*, **131**, 183–200.

1105 Swiecicki, T., Wilcockson, P., Canham, A., Whelan, G. & Homann, H. 1995. Dating,
1106   correlation and stratigraphy of the Triassic sediments in the West Shetlands area.
1107   *Geological Society Special Publication*, **91**, 57–85.

1108 Tate, M.P. & Dobson, M.R. 1989. Late Permian to early Mesozoic rifting and sedimentation
1109   offshore NW Ireland. *Marine and Petroleum Geology*, **6**, 49–59.

1110 Texaco 1978. Well 13/3-1 Final Geological Report. Texaco Ireland Ltd., compiled by Stuart,
1111   I.A.

1112 Thomson, A. & McWilliam, A. 2001. The structural style and evolution of the Bróna Basin.
1113   *Geological Society, London, Special Publications*, **188**, 401–410.

1114 Trueblood, S. and Morton, N. 1991. Comparative Sequence Stratigraphy and Structural
1115   Styles of the Slyne Trough and Hebrides Basin. *Journal of the Geological Society*, **148**,
1116   197–201, https://doi.org/10.1144/gsjgs.148.1.0197.

1117 Trueblood, S. 1992. Petroleum geology of the Slyne Trough and adjacent basins. *Geological*
1118   *Society Special Publication*, 315–326.

1119 Tyrrell, S., Haughton, P.D.W. & Daly, J.S. 2007. Drainage reorganization during breakup of
1120   Pangea revealed by in-situ Pb isotopic analysis of detrital K-feldspar. *Geology*, **35**,
1121   971–974.

1122 Tyrrell, S., Souders, A.K., Haughton, P.D.W., Daly, J.S. & Shannon, P.M. 2010.
1123   Sedimentology, sandstone provenance and palaeodrainage on the eastern Rockall
1124   Basin margin: evidence from the Pb isotopic composition of detrital K-feldspar.
1125   *Geological Society, London, Petroleum Geology Conference series*, **7**, 937–952.

1126 Van Hoorn, B. 1987. The south Celtic Sea/Bristol Channel Basin: origin, deformation and
1127   inversion history. *Tectonophysics*, **137**, https://doi.org/10.1016/0040-1951(87)90325-8.

1128 Walsh, A., Knag, G., Morris, M., Quinquis, H., Tricker, P., Bird, C. & Bower, S. 1999.
1129   Petroleum geology of the Irish Rockall Trough – a frontier challenge. *Petroleum*
1130   *Geology of Northwest Europe: Proceedings of the 5th Conference*, 433–444.

1131   Wilson, R.C.L., Hiscott, R.N., Willis, M.G. & Gradstein, F.M. 1989. The Lusitanian Basin of
1132   west-central Portugal: Mesozoic and Tertiary tectonic, stratigraphic, and subsidence
1133   history. *Extensional tectonics and stratigraphy of the North Atlantic margins*, 341–361.

1134   Withjack, M.O. & Callaway, S. 2000. Active normal faulting beneath a salt layer: An
1135   experimental study of deformation patterns in the cover sequence. *AAPG Bulletin*, **84**,
1136   627–651.

1137   Zamora, G., Fleming, M. & Gallastegui, J. 2017. Salt Tectonics Within the Offshore Asturian
1138   Basin. *In*: *Permo-Triassic Salt Provinces of Europe, North Africa and the Atlantic
1139   Margins*. Elsevier, 353–368.

1140   Figure Captions
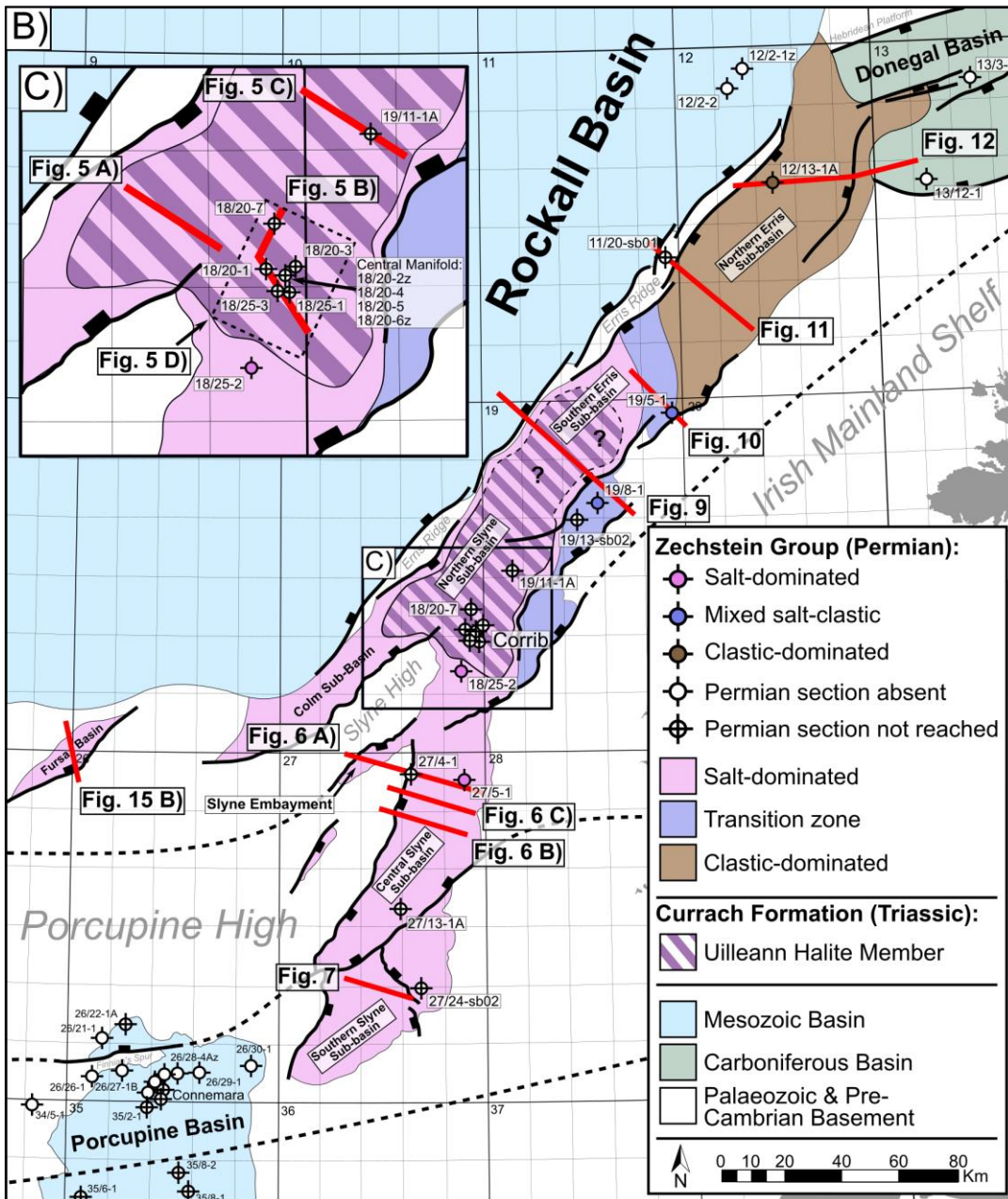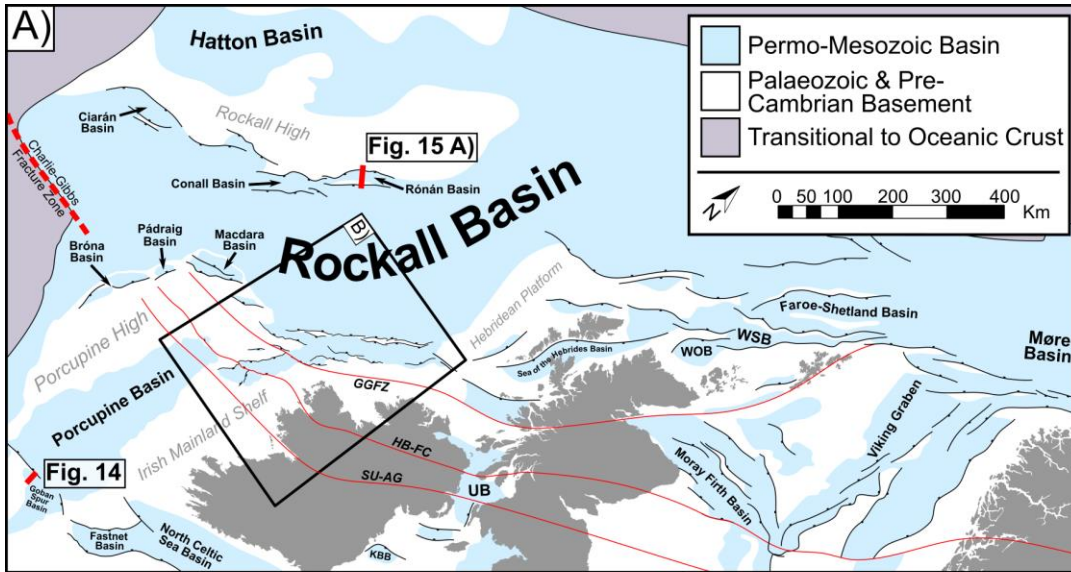
1142　**Figure 1: A)** *Map showing the location of the study area and other Permo-Mesozoic basins*

1143　*along the north-western European Atlantic margin, adapted from Doré et al. (1999) and Naylor*

1144　*et al. (1999). Caledonian structural lineaments which segment the basins are highlighted in*

1145　*red.* **Abbreviations:** *GGFZ – Great Glen Fault Zone; HB-FC – Highland Boundary-Fair Head-*

1146　*Clew Bay Lineament; KBB – Kish Bank Basin; SU-AG – Southern Uplands-Antrim-Galway*

1147　*Lineament; UB – Ulster Basin; WOB – West Orkney Basin; WSB – West Shetland Basin.* **B)**

1148　*Map showing the distribution of Permian and Triassic salt throughout the Slyne and Erris*

1149　*basins and neighbouring basins. Faults are displayed at Top Permian offset.* **C)** *Map showing*

1150　*distribution of salt in the Northern Slyne Sub-basin.*
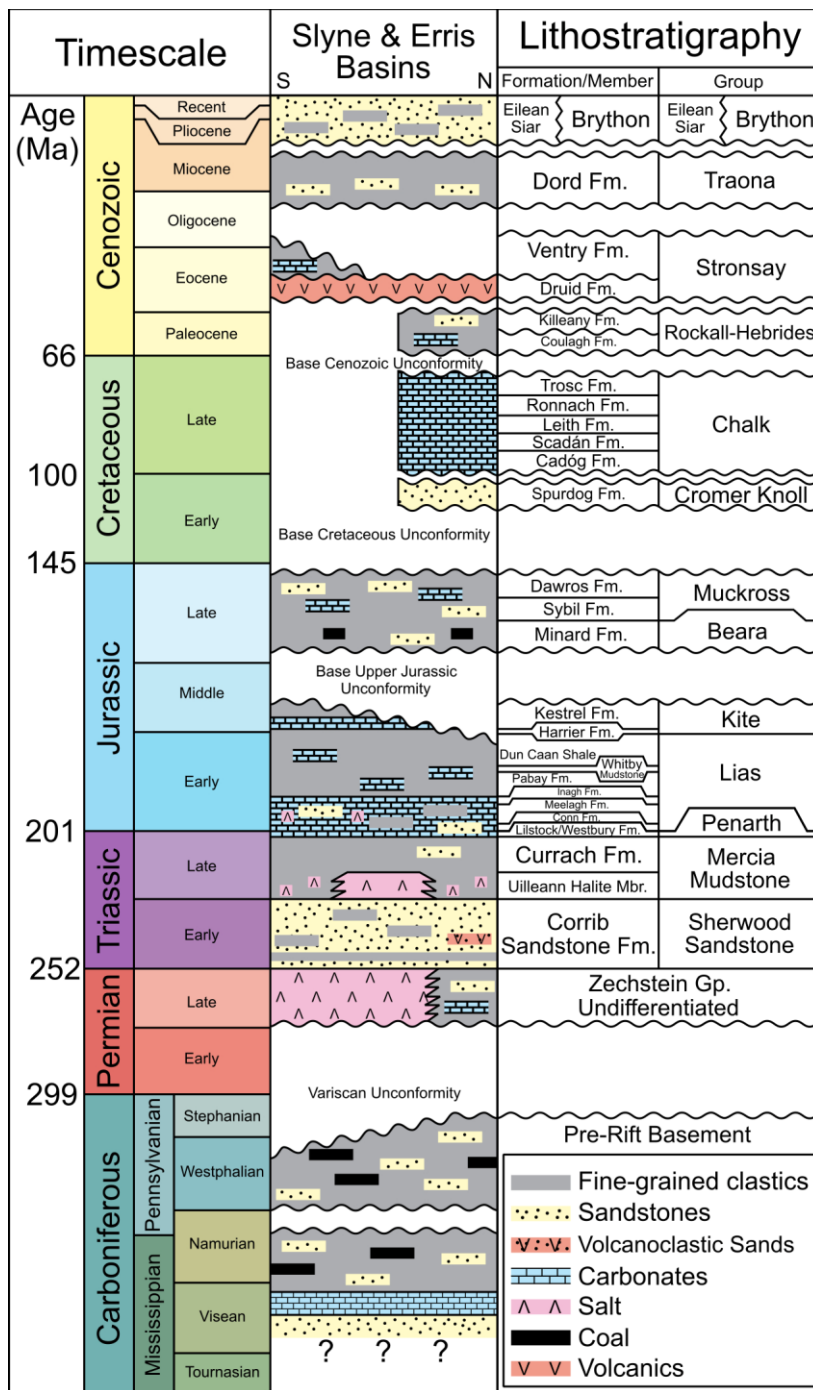
1151

Figure 2: Simplified chronostratigraphic chart for the Slyne and Erris basins. Lithostratigraphic nomenclature adapted from Merlin Energy Resources Consortium (2020).
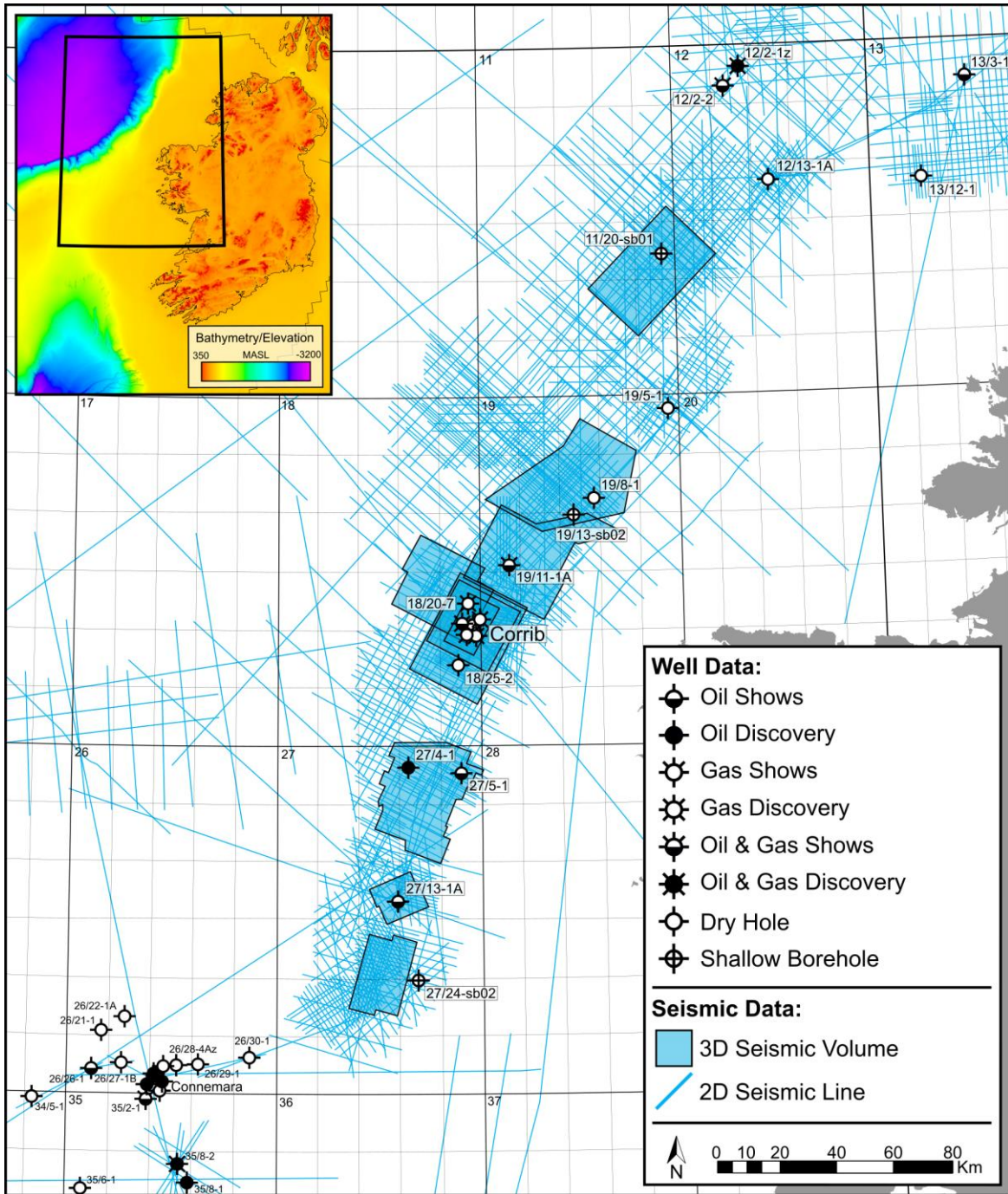
1154

1155   **Figure 3:** *Map showing study area and datasets used.* **Inset Map:** *Bathymetry of the study*

1156   *area.*
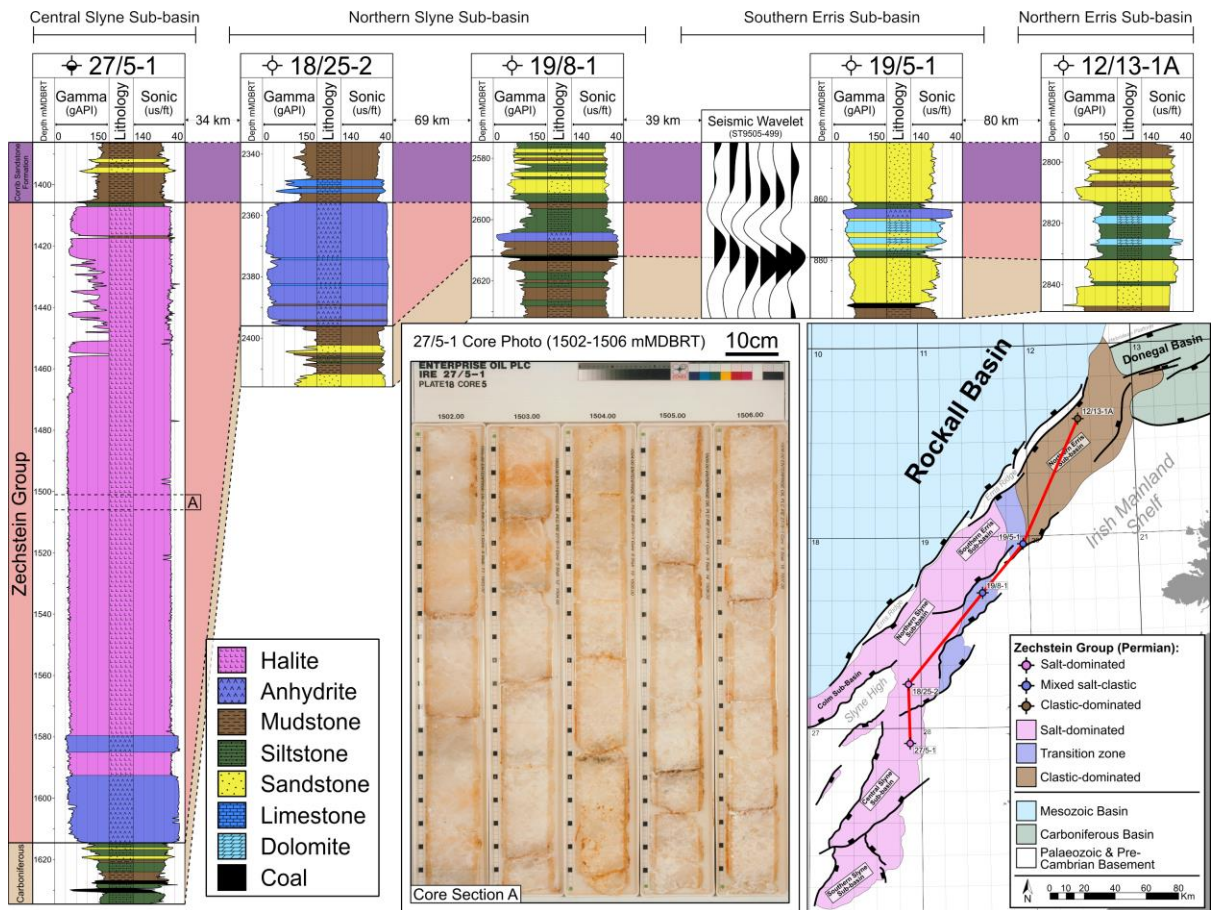
Figure 4: *Lithological well correlation of the Zechstein Group through the Slyne and Erris basins. Correlation is flattened to the top of the Zechstein Group.* **Inset:** *Select core photos from the 27/5-1 well in the central Slyne Basin, showing the massive, crystalline, halite-prone Zechstein Group.*
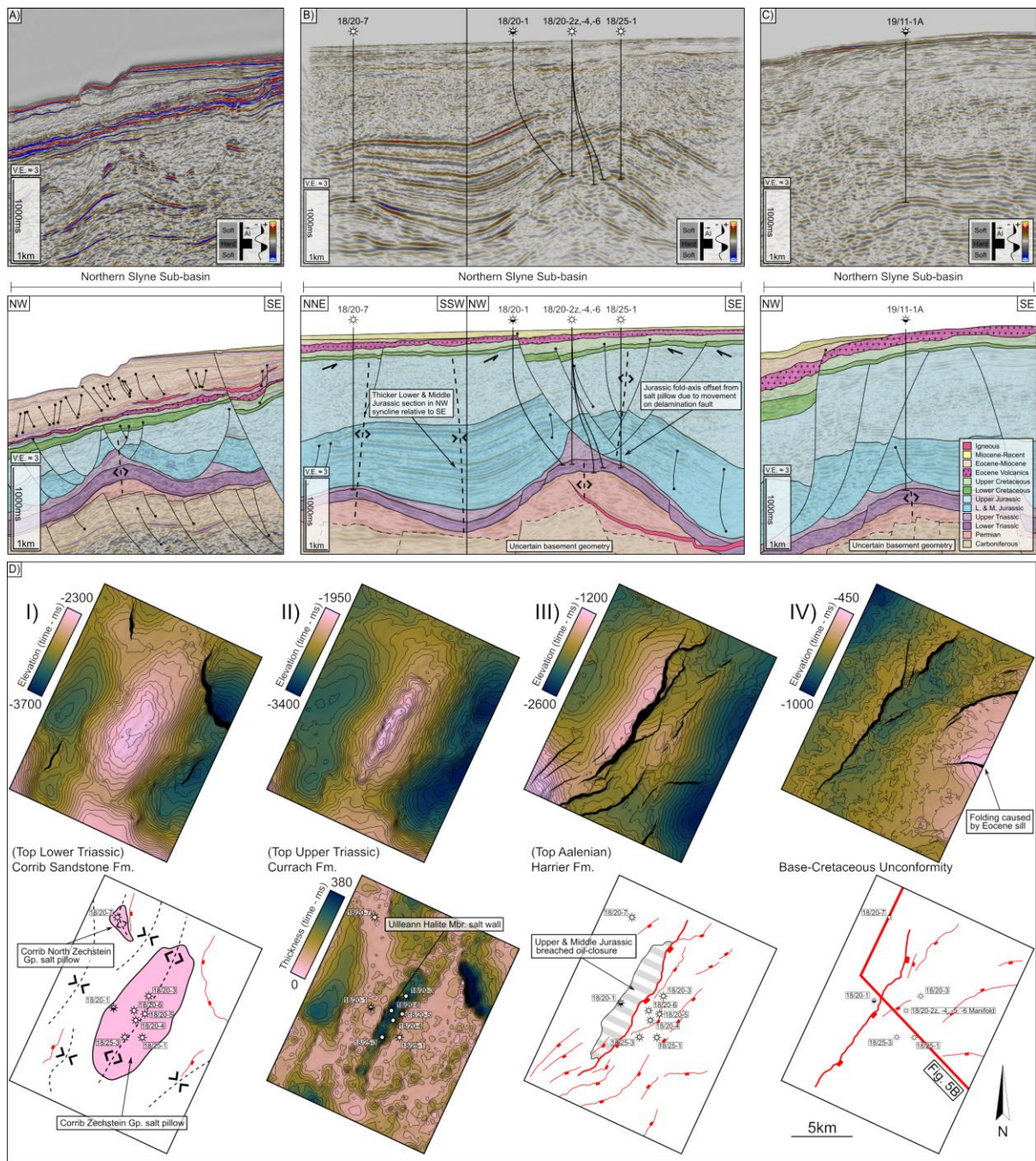
1162

Figure 5: *Seismic sections from the northern Slyne Basin. See figure 1 for locations.* **A)** *Inline 1600 from the 2018 Inishkea Reprocessed 3D seismic volume and accompanying geoseismic section. A Zechstein Group salt pillow folds the Corrib Sandstone Formation, with delamination faults soling out in the Uilleann Halite Member of the Currach Formation above the crest of the fold.* **B)** *Arbitrary line from the 2013-01 (13SH3D) 3D seismic volume and accompanying geoseismic interpretation. Two salt-cored folds are visible, one containing the 18/20-7 'Corrib North' gas discovery, and the other containing the Corrib gas field. A major eastward-dipping delamination fault is developed in the Jurassic section above the crest of the Corrib structure, soling out above a small salt diapir within the Uilleann Halite Member, with a faulted rollover*

1172 *formed in the hanging-wall of this fault. Well name 18/20-2z, -4, -6 indicates the location of the*

1173 *subsea manifold for three distinct wells. **C)** Arbitrary line from the 2001/01 3D seismic volume*

1174 *and accompanying geoseismic section. The salt-cored fold tested by the 19/11-1A well is*

1175 *shown, with minor delamination faults forming above, soling out in the Uilleann Halite Member*

1176 *The steep westward dip along the western edge of the structure demonstrates the influence*

1177 *of post-rift thermal subsidence in the Rockall Basin. **D) I)** Time-structure map of the top Corrib*

1178 *Sandstone Formation and accompanying map (below) showing Zechstein Group salt pillows.*

1179 ***II)** Time-structure map of the top Currach Formation and accompanying TWTT thickness map*

1180 *(below) of the Currach Formation. **III)** Time-structure map of the Top Harrier Formation and*

1181 *accompanying fault map (below) with the maximum structural closure in the hanging-wall*

1182 *highlighted (the extent of the residual column encountered in well 18/20-1 is uncertain). **IV)***

1183 *Time-structure map of the Base-Cretaceous Unconformity and accompanying fault map*

1184 *(below).*
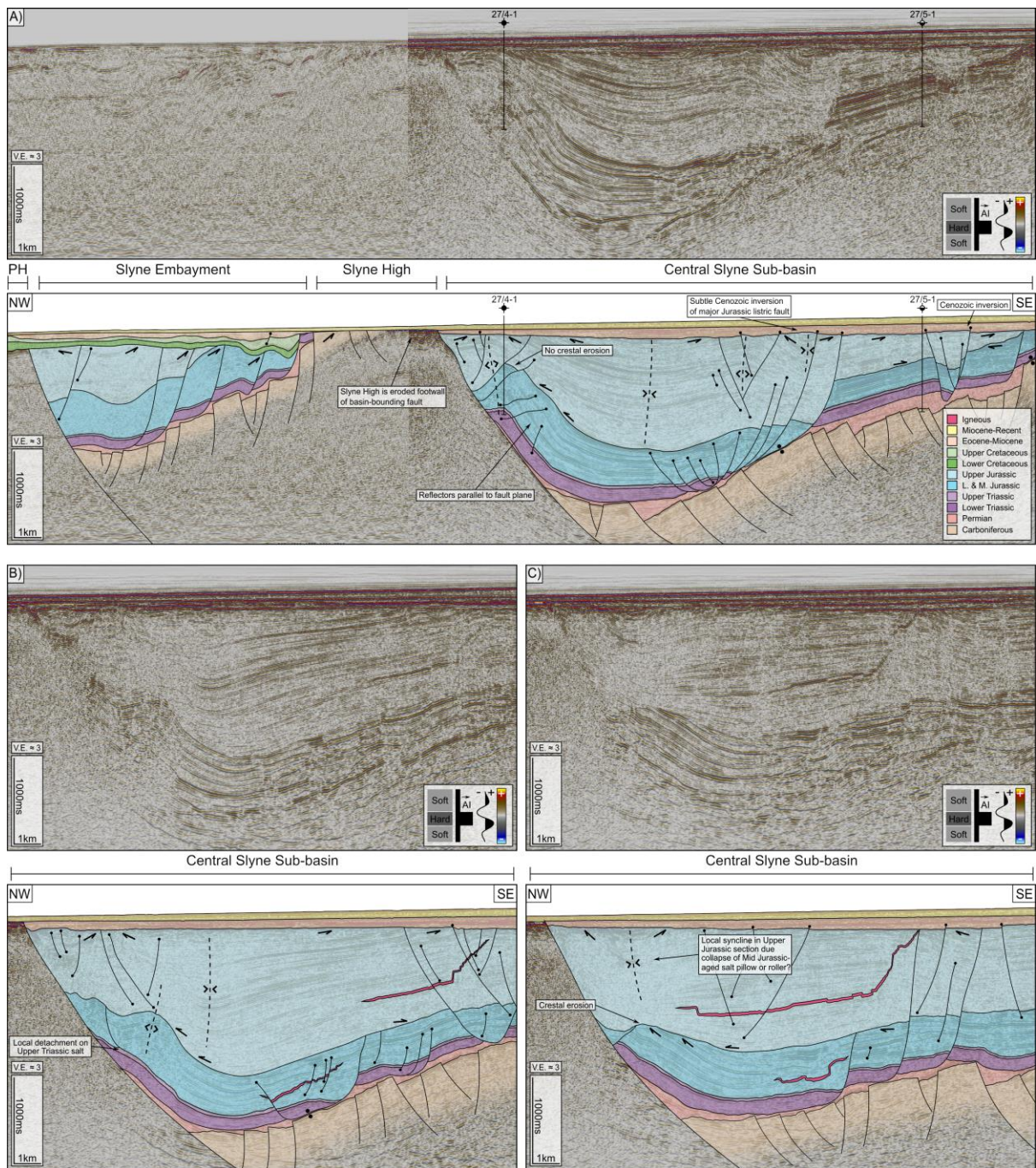
1185

Figure 6: *Seismic sections from the central Slyne Basin. See figure 1 for seismic line locations.* **A)** *Composite seismic section of 2D seismic line E96IE09-28 and inline 2740 from the 2000/08 (E00IE09) 3D seismic volume with accompanying seismic interpretation.* **Abbreviations:** *PH – Porcupine High* **B)** *Inline 1790 from the 2000/08 (E00IE09) 3D seismic volume with accompanying seismic interpretation.* **C)** *Inline 2040 from the 2000/08 (E00IE09) 3D seismic volume with accompanying seismic interpretation.*
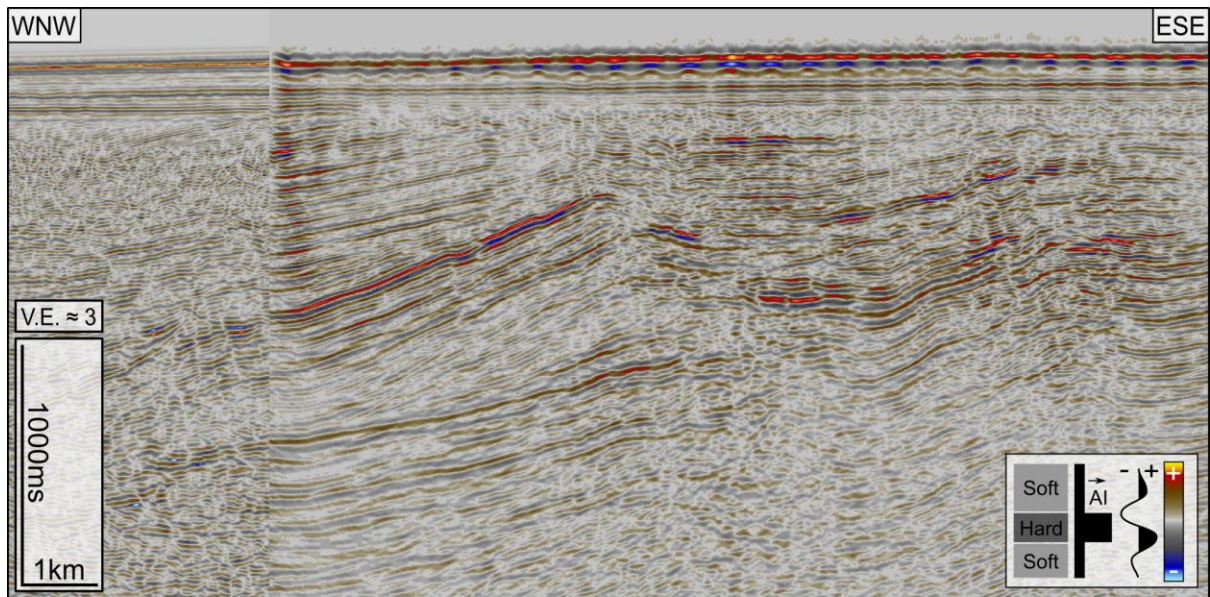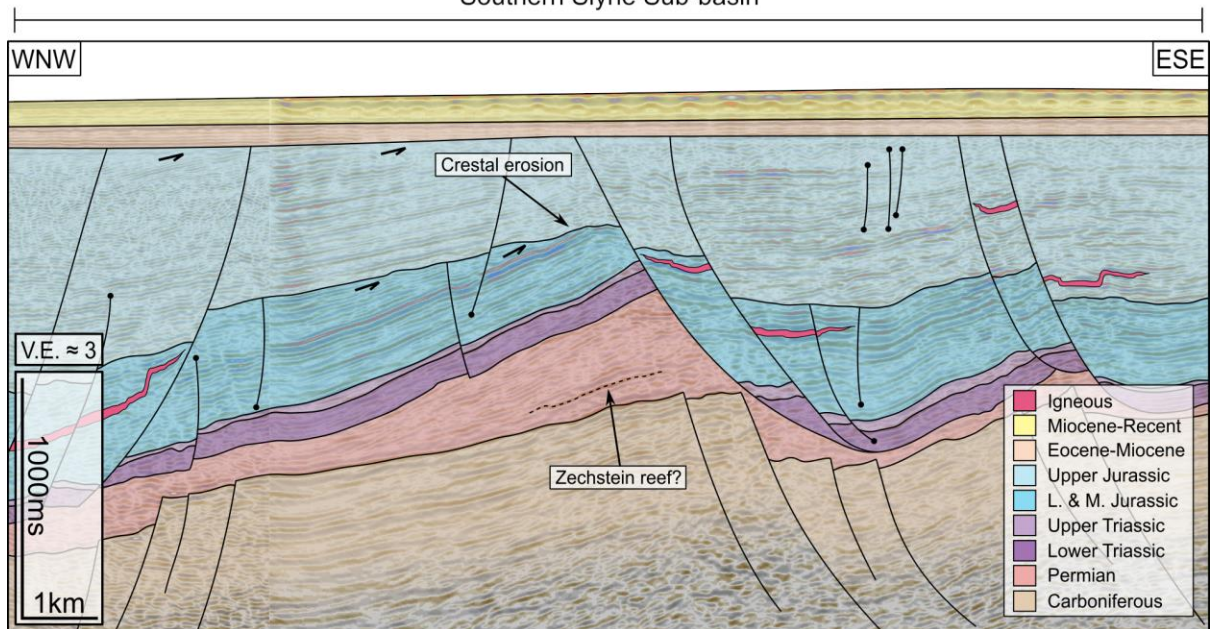
1192

Figure 7: Composite seismic section of 2D seismic line TK25-95-32 and crossline 3163 from the 2010/01 (SL103D) 3D seismic volume, with accompanying geoseismic interpretation. The Middle and Lower Jurassic section is severely eroded on the crest of the fault block cored by the large salt roller, with a thicker section preserved in the hanging-wall. See figure 1 for seismic line location.
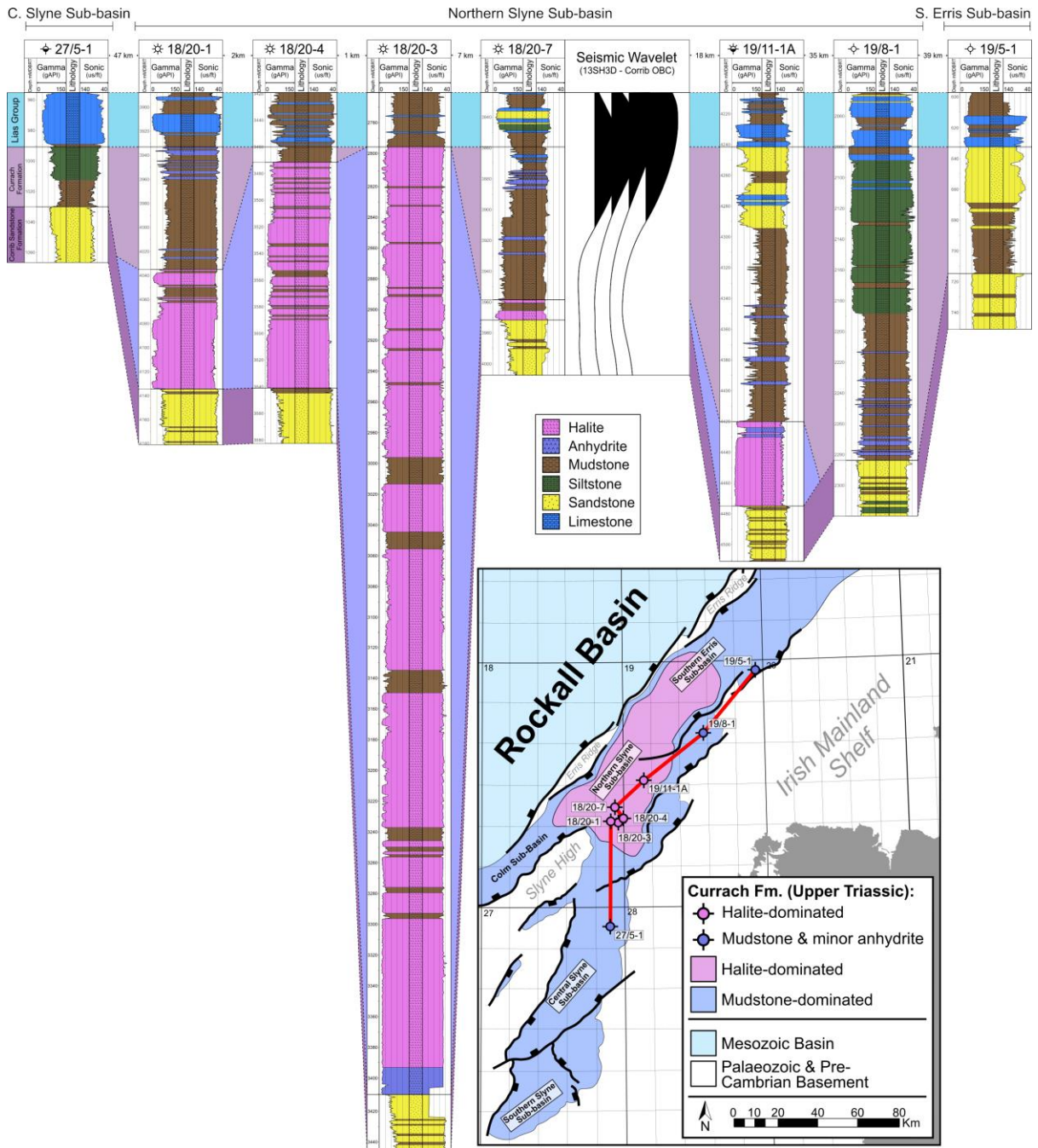
Figure 8: *Lithological correlation of the Currach Formation and Uilleann Halite Member of select wells through the Slyne and Erris basins. Correlation is flattened to the top of the Currach Formation. Well 18/20-3 penetrates the salt wall above the Corrib salt-cored fold.*
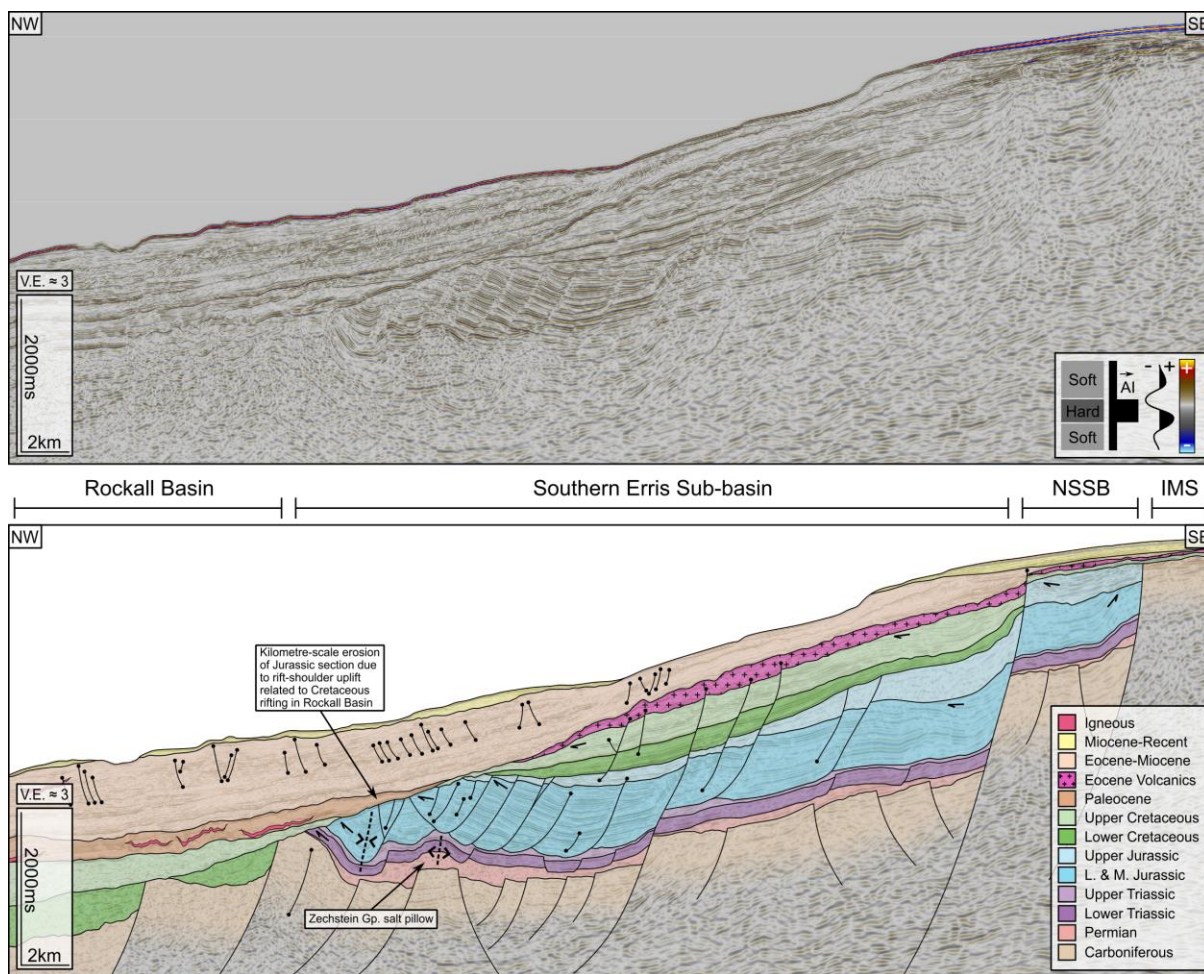
1202

Figure 9: *2D seismic line ERM07-6000 and accompanying geoseismic section. The Jurassic section in the southern Erris Basin is dominated by tightly spaced, westward-dipping listric faults which detach on the Uilleann Halite Member. There is also a Zechstein salt pillow evident near the western margin of the basin. Stratigraphy in the Rockall Basin is constrained through correlation with the 12/2-1 and 12/2-2 wells to the NE. See figure 1 for seismic line location.* **Abbreviations:** *IMS – Irish Mainland Shelf; NSSB – Northern Slyne Sub-basin.*
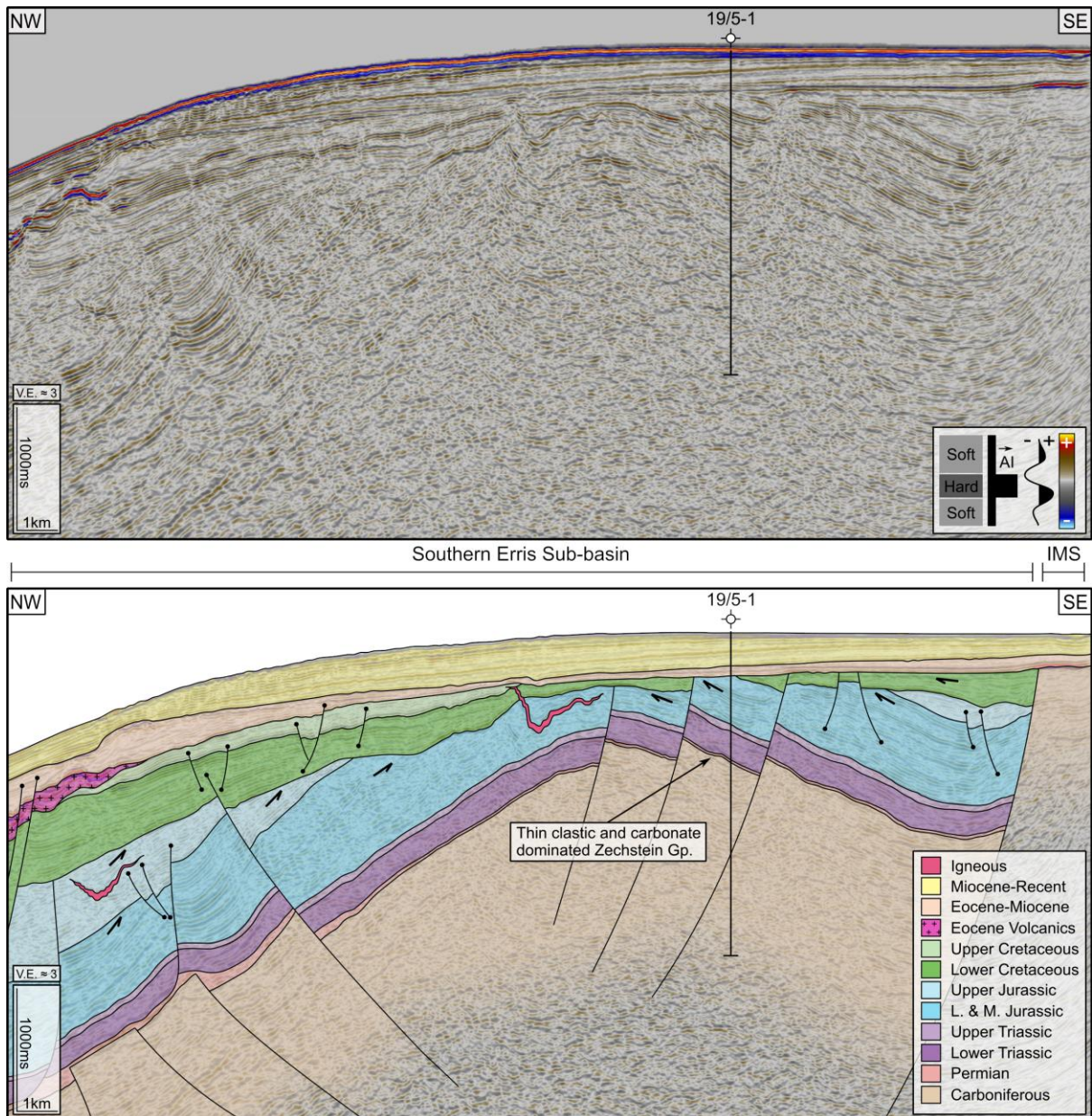
1209

Figure 10: *2D seismic line ST9505-449 and accompanying geoseismic section. The proportion of salt in the Zechstein Group increase north-westwards. Faults on the eastern side of the section hard link through the Zechstein Group, while on the western side faults are mechanically detached above and below the Zechstein Group salt. See figure 1 for seismic line location.* Abbreviations: *IMS – Irish Mainland Shelf.*
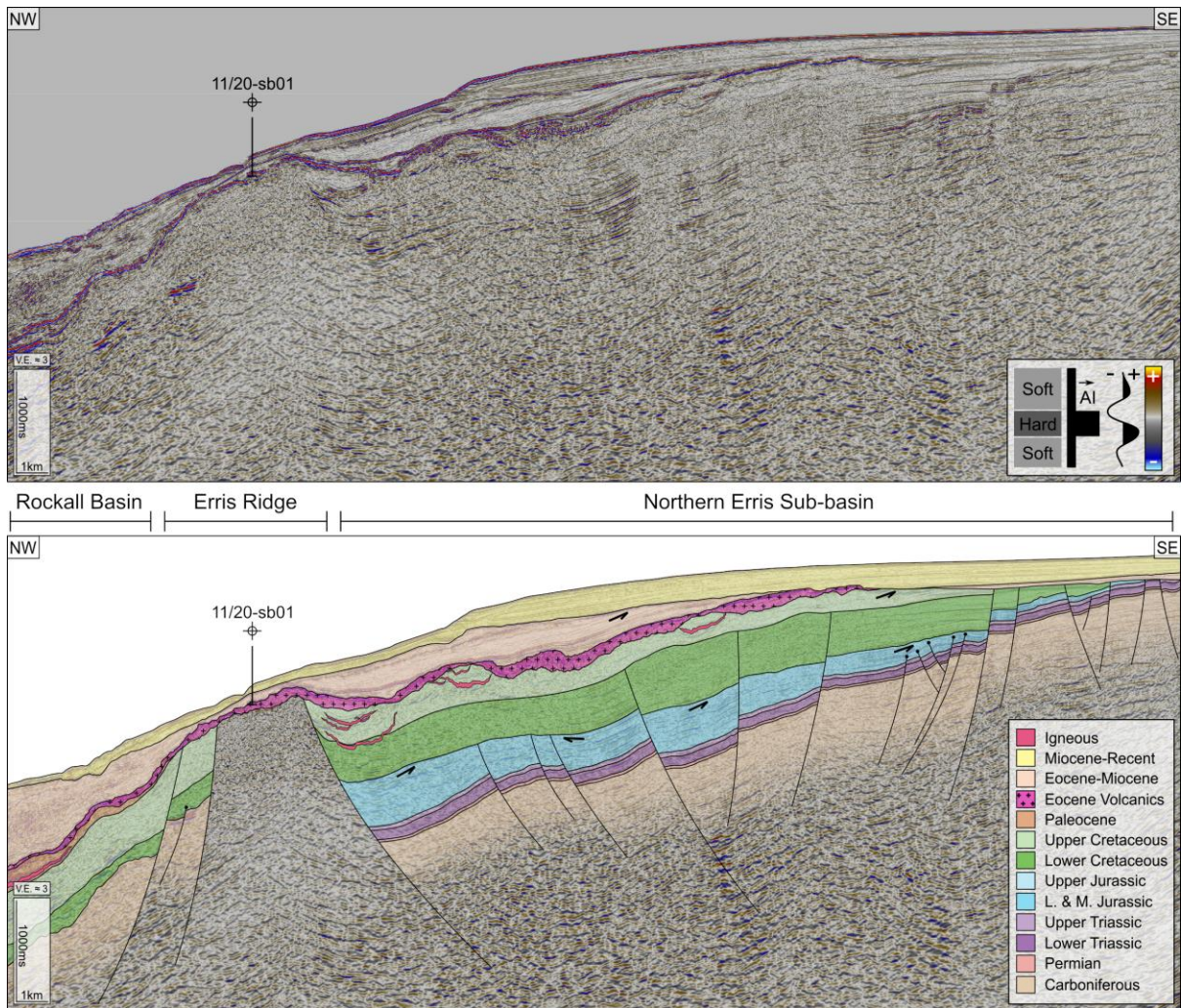
1215

Figure 11: *2D seismic line PH98GPO133-027 and accompanying geoseismic section. The northern Erris Basin dips westwards into the bounding fault along the margin of the Erris Ridge, with a significantly reduced Mesozoic section preserved beneath the Base-Cretaceous Unconformity. There is little evidence of salt-related structures in this part of the basin. Eocene lavas cause significant degradation of image quality. See figure 1 for seismic line location.*
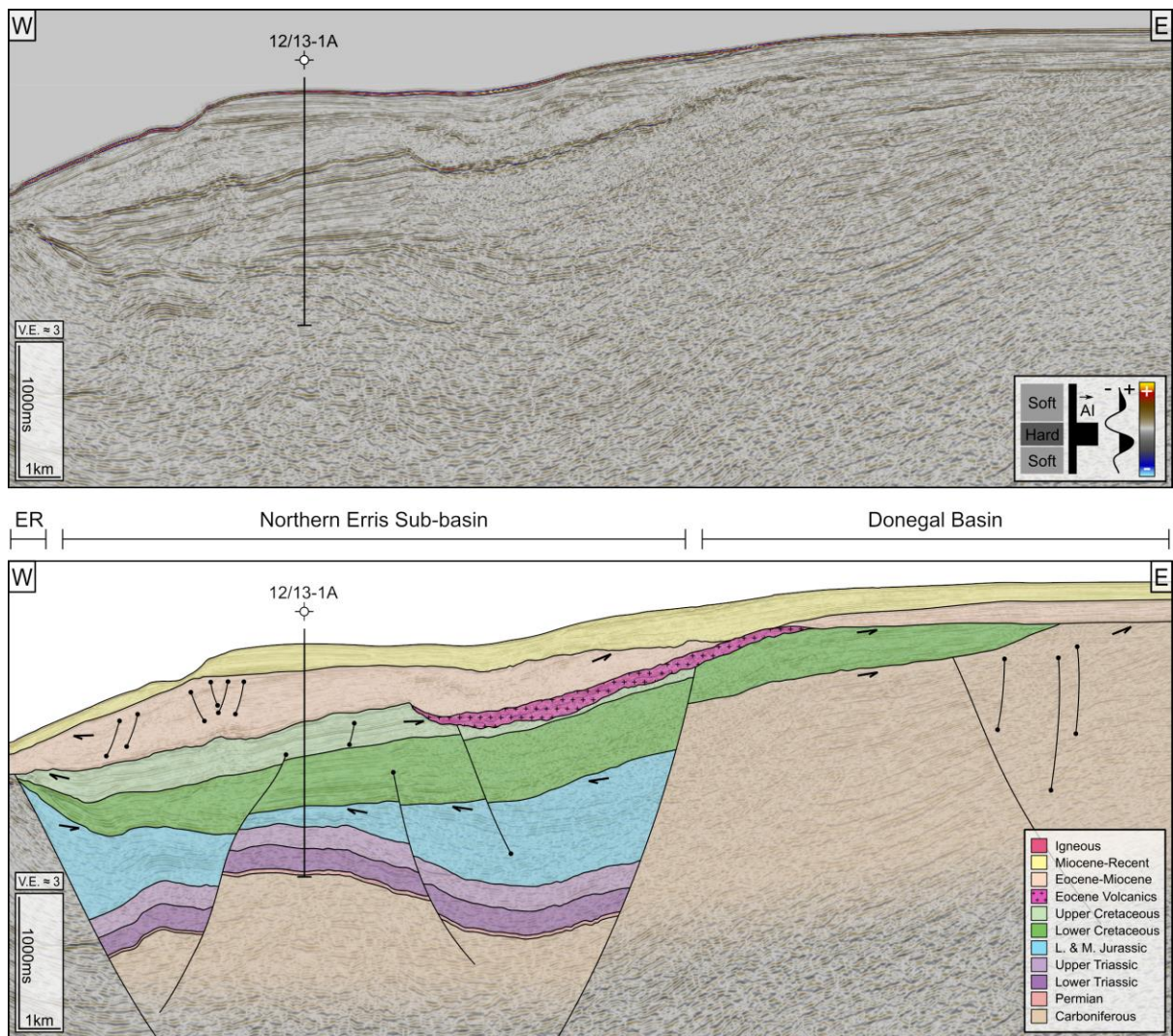
1221

Figure 12: 2D seismic line DBS99-304 and accompanying geoseismic section. Here the northern Erris Basin is bounded by the Erris Ridge to the northwest and the Palaeozoic Donegal Basin to the northeast, with a significantly reduced Mesozoic section preserved beneath the BCU. There is little evidence of salt-related structures in this part of the basin. See figure 1 for seismic line location. *Abbreviations:* ER – Erris Ridge.

Timescale	Southern Slyne Sub-basin	Central Slyne Sub-basin	Northern Slyne Sub-basin
Cenozoic	· Regional uplift & erosion · Emplacement of sills (NAIP)	· Regional uplift & erosion · Minor extension	· Regional uplift & erosion · Extrusion of lava · Emplacement of sills (NAIP)
Cretaceous	· Regional kilometre-scale uplift & erosion	· Regional kilometre-scale uplift & erosion · Minor extension	· Regional kilometre-scale uplift & erosion
Late Jurassic	· Regional extension · Reactivation & continued growth of reactive diapir	· Regional extension · Emergence of Slyne High as footwall of major fault · Possible formation of salt wall above the Slyne High	· Regional extension · Reversal of salt pillow polarity · Thicker Upper Jurassic section in SE syncline
Mid Jurassic (Bathonian-Callovian)	· Regional uplift & erosion · Sharp truncation at crest of structure	· Regional uplift & erosion	· Regional uplift & erosion
Mid Jurassic (Aalenian-Bajocian)	· Continued regional extension · Continued growth of salt roller	· Continued regional extension	· Continued growth of Permian salt pillow · Initiation of delamination fault & Triassic salt roller
Early Jurassic	· Initiation of regional extension & Permian salt roller	· Initiation of regional extension & halokinesis · Growth sequences in hanging-walls above Permian salt rollers	· Initiation of regional extension · Initiation of Permian salt pillow · Thicker Lower Jurassic section in NW syncline relative to SE syncline

1227

Figure 13: Schematic evolutionary model for the formation of different salt-related structures discussed in this study highlighting their multiphase structural evolution. Seismic lines through the structures illustrated in the Southern, Central and Northern Slyne sub-basins are shown in Fig. 6, 7A and 8B respectively. **Abbreviations:** NAIP – North Atlantic Igneous Province.
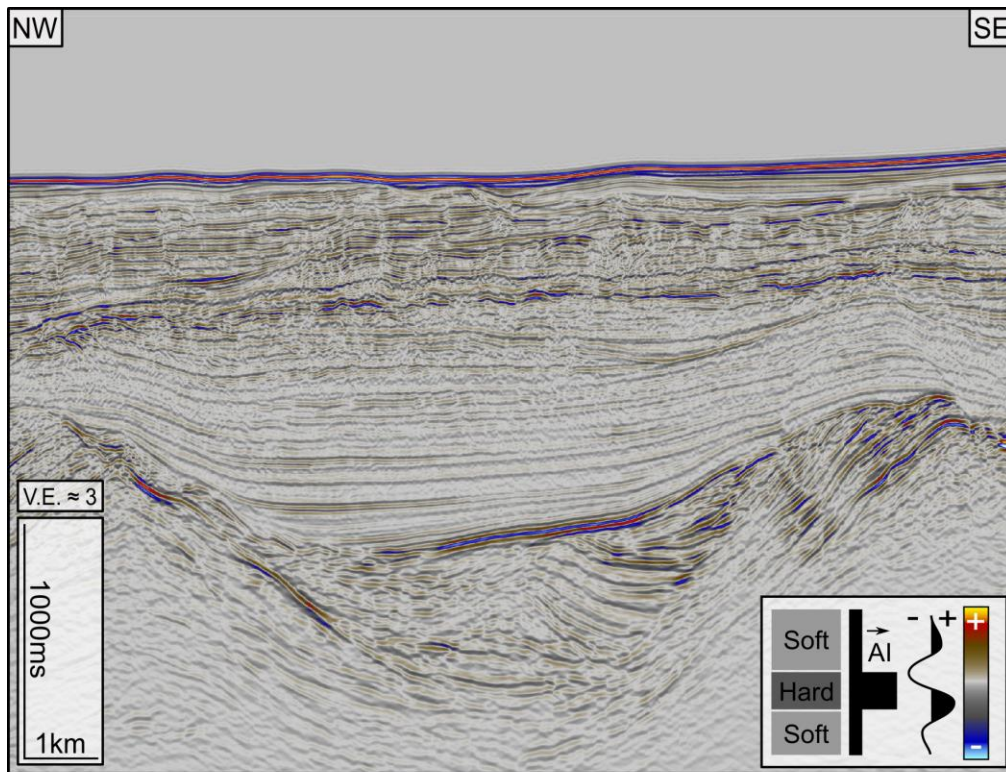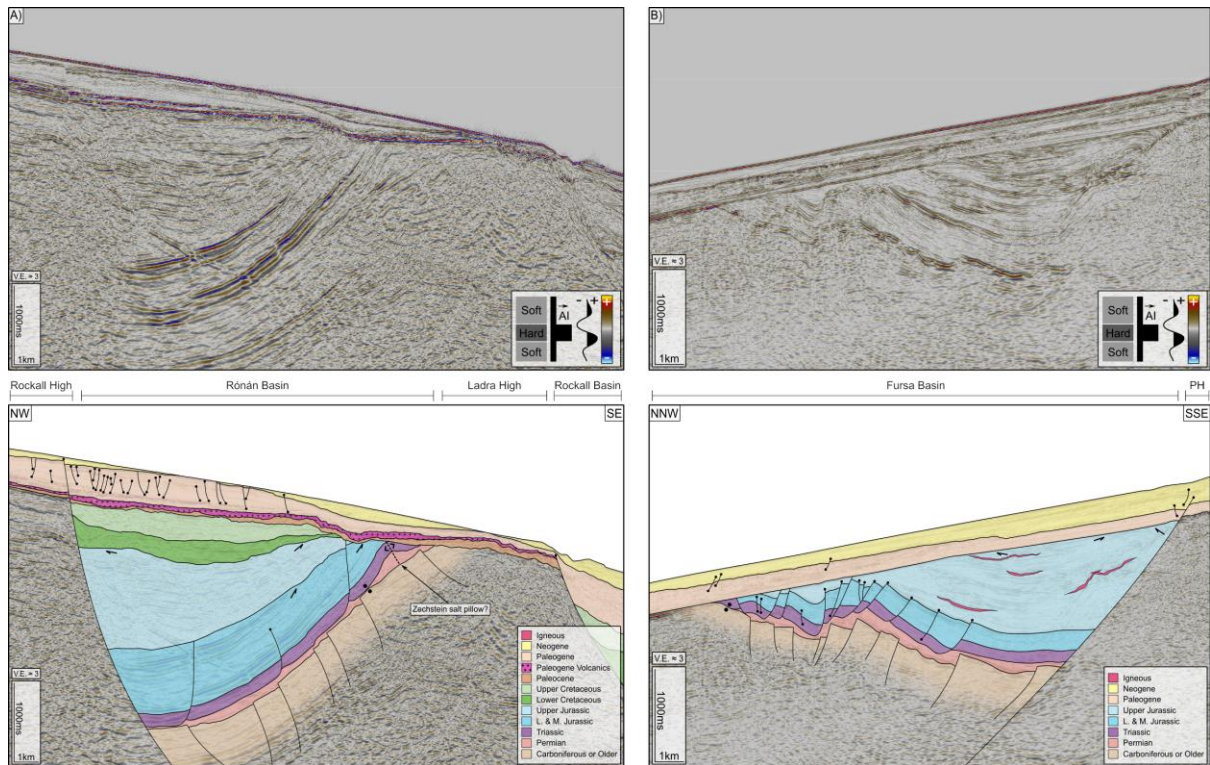
Goban Spur Basin
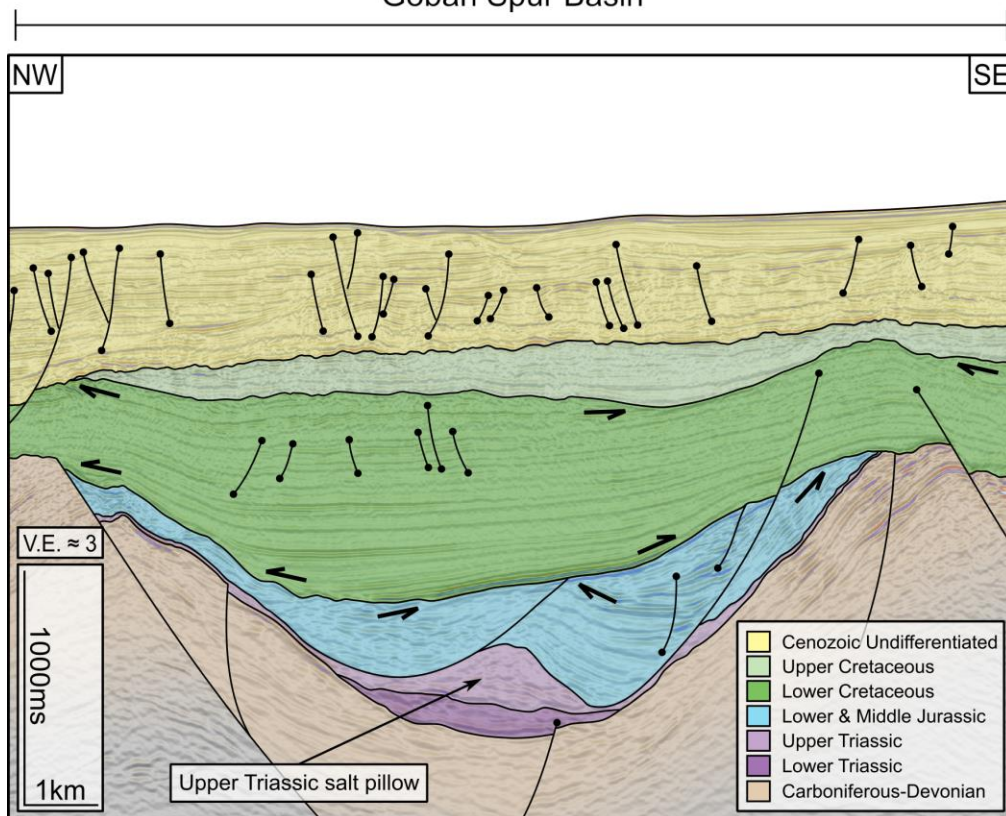
1232

Figure 14: *Part of 2D seismic line PAD13-044M and accompanying geoseismic section. A distinct décollement surface is observed beneath the Base-Cretaceous Unconformity. An Upper Triassic salt pillow is also observed in this section.*

1236

Figure 15: A) Part of 2D seismic line WRM96-107 and accompanying geoseismic section. The Rónán Basin is located on the 'conjugate margin' of the Erris Basin on the north-western margin of the Rockall Basin. B) Part of 2D seismic line IR11040 and accompanying geoseismic section. A distinct décollement surface is interpreted in the Fursa Basin between the bright top-basement reflector and the overlying Mesozoic section. Abbreviations: PH – Porcupine High. Note: As the Rónán and Fursa basins are currently undrilled, these interpretations are speculative.
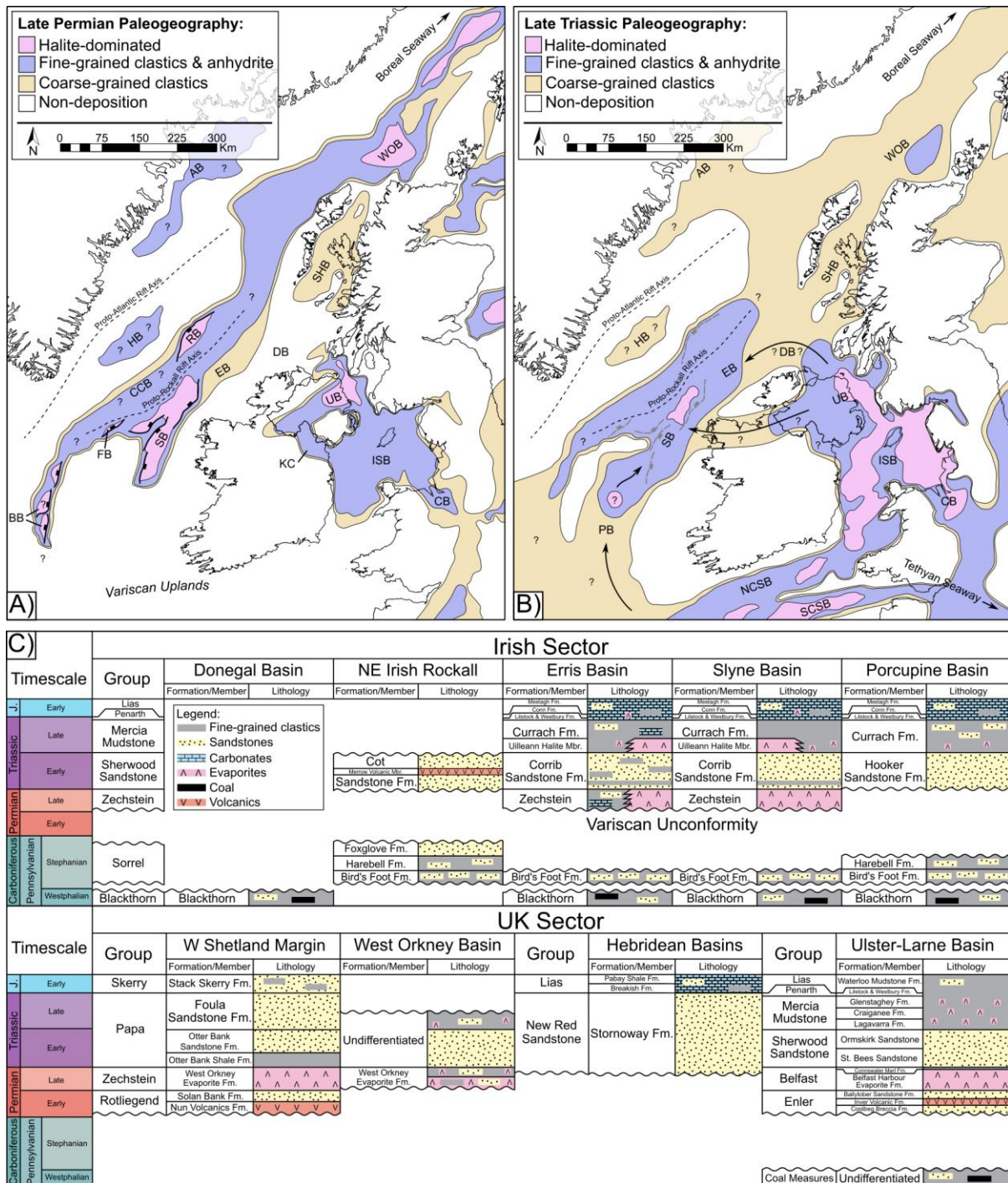
1244

Figure 16: A) *Schematic Late Permian paleogeographic map of the Irish Atlantic margin and neighbouring regions showing the route of marine ingress from the Boreal Ocean to the Slyne and Erris basins.* **B)** *Schematic Late Triassic paleogeographic map of the Irish Atlantic margin and neighbouring regions showing three potential routes of marine ingress from the Tethys Ocean to the Slyne and Erris basins. UK sector, Irish Sea and Celtic Sea basins adapted from McKie, 2017. Greenland basins adapted from Gerlings et al., 2017.* **C)** *Simplified stratigraphic columns of the Upper Pennsylvanian to Lower Jurassic sections from several basins surrounding the study area, showing the broad distribution and composition of Permo-Triassic*

1253   *rocks. Irish sector adapted from Merlin Energy Resources Consortium (2020), UK sector*

1254   *adapted from Stoker et al. (2017), Ulster-Larne Basin adapted from Quinn et al. (2010).*

1255   ***Abbreviations:*** *AB – Ammassalik Basin; BB – Bróna basins; CB – Cheshire Basin; EB – Erris*

1256   *Basin; FB – Fursa Basin; HB – Hatton Basin; ISB – Irish Sea basins; KC – Kingscourt; NCSB*

1257   *– North Celtic Sea Basin; PB – Porcupine Basin; RB – Rónán Basin; SB – Slyne Basin; SCSB*

1258   *– South Celtic Sea Basin; SHB – Sea of the Hebrides Basin; UB – Ulster Basin; WOB – West*

1259   *Orkney Basin.*